Cellular and Molecular Life Sciences (2020) 77:4143–4161
https://doi.org/10.1007/s00018-019-03412-x

ORIGINAL ARTICLE

Dynein-mediated nuclear translocation of yes-associated protein through microtubule acetylation controls fibroblast activation

Eunae You[1] · Panseon Ko[1] · Jangho Jeong[1] · Seula Keum[1] · Jung-Woong Kim[1] · Young-Jin Seo[1] · Woo Keun Song[2] · Sangmyung Rhee[1]

Received: 12 July 2019 / Revised: 27 November 2019 / Accepted: 4 December 2019 / Published online: 7 January 2020

Abstract

Myofibroblasts are the major cell type that is responsible for increase in the mechanical stiffness in fibrotic tissues. It has well documented that the TGF-β/Smad axis is required for myofibroblast differentiation under the rigid substrate condition. However, the mechanism driving myofibroblast differentiation in soft substrates remains unknown. In this research, we demonstrated that interaction of yes-associated protein (YAP) and acetylated microtubule via dynein, a microtubule motor protein drives nuclear localization of YAP in the soft matrix, which in turn increased TGF-β1-induced transcriptional activity of Smad for myofibroblast differentiation. Pharmacological and genetical disruption of dynein impaired the nuclear translocation of YAP and decreased the TGF-β1-induced Smad activity even though phosphorylation and nuclear localization of Smad occurred normally in α-tubulin acetyltransferase 1 (α-TAT1) knockout cell. Moreover, microtubule acetylation prominently appeared in the fibroblast-like cells nearby the blood vessel in the fibrotic liver induced by CCl_4 administration, which was conversely decreased by TGF-β receptor inhibitor. As a result, quantitative inhibition of microtubule acetylation may be suggested as a new target for overcoming fibrotic diseases.

Keywords Myofibroblast · TGF-β1 · ECM stiffness · Microtubule acetylation · Liver fibrosis · YAP · Smad

Abbreviations

ECM	Extracellular matrix
MEFs	Mouse embryonic fibroblasts
α-TAT1	α-Tubulin acetyltransferase 1
TGF-β1	Transforming growth factor beta1
α-SMA	Alpha-smooth muscle actin
EHNA	Erythro-9-(2-hydroxy-3-nonyl)adenine
FMC	Floating matrix contraction
SMC	Stressed matrix contraction
YAP	Yes-associated protein
CCl_4	Cabon tetrachloride
PTMs	Post-translational modifications
ICC	Immunocytochemistry
IHC	Immunohistochemistry

Electronic supplementary material The online version of this article (https://doi.org/10.1007/s00018-019-03412-x) contains supplementary material, which is available to authorized users.

✉ Woo Keun Song
wksong@gist.ac.kr

✉ Sangmyung Rhee
sangmyung.rhee@cau.ac.kr

[1] Department of Life Science, Chung-Ang University, Seoul 06974, Republic of Korea

[2] Bio Imaging and Cell Logistics Research Center, School of Life Sciences, Gwangju Institute of Science and Technology, 123 Cheomdangwagi-ro, Buk-Gu, Gwangju 61005, Republic of Korea

Introduction

Differentiation and phenotypical plasticity of cells are critically dependent on the nature of the cellular microenvironment [1, 2]. The cellular microenvironment is composed of various types of extracellular matrix (ECM) proteins, soluble growth factors, and numerous type of cells [3, 4]. The ECM proteins, which surround cells, play particularly important roles as mechanical supporters of the cells. Depending on the nature of the tissue, ECM proteins exhibit different mechanical properties with respect to the cells that constitute the tissue [1, 5]. The ability of cells to sense the mechanical properties of ECM is essential for maintaining tissue homeostasis. Disruption of tissue homeostasis by pathological processes, including tissue injury, inflammation, and cancer, is accompanied by mechanical degeneration such as fibrosis

[6]. In this environment, the mechanically stiffened tissue allows cells to be more active, resulting in acceleration of pathological progression [7, 8].

Fibroblasts maintain the mechanical properties of ECM by regulating the tensional status of tissues [9]. When a tissue is under pathological conditions, pro-fibrotic agonists, such as transforming growth factor-beta1 (TGF-β1), are secreted from the surrounding immune cells to promote the differentiation of fibroblasts into myofibroblasts [10]. The differentiated myofibroblasts actively participate in innate stromal remodelling by changing the composition and mechanical properties of ECM during pathological progression. In fact, the number of myofibroblast expressing the alpha-smooth muscle actin (α-SMA) as a contractile apparatus has increased in the pathological tissues including idiopathic pulmonary fibrosis (IPF), liver fibrosis, cardiovascular fibrosis and systemic sclerosis [11, 12]. Consequently, in fibrotic tissue, an increase in tissue rigidity by myofibroblasts is the main cause of organ failure and death. Thus, understanding the mechanism of myofibroblast differentiation is important in the study of disease progression [13, 14]. Numerous studies have shown that ECM stiffness, in addition to biochemical agonists, is required for myofibroblast differentiation [15]. Normal lung fibroblasts cultured in stiff substrates (~20 kPa; lung fibrotic rigidity) without agonist, acquire a myofibroblastic phenotype including α-SMA expression than soft substrates (~0.5 kPa; normal lung rigidity), which is induced by integrin-mediated mechanotransduction pathway [16-19]. However, because early pathological tissues are as soft as normal tissues, the signalling pathways associated with myofibroblast differentiation in soft substrates may differ from those occurring in stiff substrates. Nevertheless, the molecular mechanisms driving myofibroblast differentiation in soft substrates remain unclear. We have also recently found that mouse embryonic fibroblasts (MEFs) with knockout (KO) of the *Spin90* gene show increased microtubule acetylation and myofibroblastic phenotype in a 0.5 kPa polyacrylamide gel (PAG) substrate that mimics normal tissue stiffness, indicating that microtubules may be involved in myofibroblast differentiation under soft substrate conditions [20]. However, whether microtubule dynamics are required for myofibroblast differentiation under pathological conditions remains to be elucidated.

Yes-associated protein (YAP) is a key regulator of myofibroblast in response to ECM stiffness [15, 21]. Notably, inhibition of integrin-derived cellular contractile activity via inhibition of myosin and Rho kinase activities significantly reduces YAP nuclear accumulation, indicating that YAP is activated by intrinsic mechanotransduction in response to ECM stiffening [21]. Altogether, YAP/TAZ complex mediates the mechanical stress exerted by the ECM and drives a positive-feedback loop to accelerate fibrotic disease and cancer development. Interestingly, cytoplasmic YAP under low matrix stiffness is translocated into the nucleus upon the treatment of TGF-β1 in dermal fibroblasts, suggesting the existence of a mechanism in which YAP is translocated to the nucleus when cells are grown on a soft matrix [22]. However, the underlying molecular mechanisms responsible for TGF-β1-induced nuclear entry of YAP under low matrix stiffness remain unknown.

Cellular signalling differs in 2D vs. 3D collagen matrices [9, 23], which impacts myofibroblast differentiation. In addition, microtubule acetylation is required for the myofibroblast differentiation under soft substrate condition [20]. These findings highlight the need to understand how microtubule acetylation controls the myofibroblast differentiation under soft substrate condition. In this study, we investigated the molecular mechanisms driving myofibroblast differentiation in soft matrices that mechanically mimic the early pathological stage of fibrosis.

Materials and methods

Antibodies and reagents

In this study, we used antibodies against α-SMA (Sigma-Aldrich, St Louis, MO, USA, #A5228), acetylated-α-tubulin (Cell Signaling Tech., Beverly, MA, USA, #5335), detyrosinated-α-tubulin (Millipore, Billerica, MA, USA, #MAB3201), α-tubulin (Sigma-Aldrich, #T9026), GFP (Santa Cruz Biotech., #sc-9996), pMLC (Ser 19; Abcam, Cambridge, MA, USA, #ab64162), YAP (Santa Cruz Biotech., #sc-101199), phospho-Smad2 (Ser465/467)/Smad3 (Ser423/425) (Cell Signaling Tech., #8828), Smad2/3 (Santa Cruz Biotech., #sc-133098) and dynein (Millipore, Billerica, MA, USA, #MAB1618). TGF-β1 (R&D systems, MN, USA, #240B), as well as EHNA (Tocris Bioscience, UK, #1261) and nocodazole (Sigma-Aldrich, #M1404), were used as growth factor or inhibitors.

Animal models and procedures

Male C57BL/6N mice, 6 weeks of age, were purchased from DBL (Chungcheongbuk-do, Republic of Korea). Mice were injected with vehicle (corn oil) or CCl_4 (0.5 ml kg^{-1} body weight, i.p.) twice a week for 2 or 4 weeks. SB431542 (10 mg kg^{-1} body weight, i.p.) was injected into mice twice a week for 4 weeks, 1 day before CCl_4 injection. Mice were sacrificed 2 days after the final CCl_4 injection. The Chung-Ang University Institutional Review Board (IRB) approved all procedures involving mice used in this study.

Cell culture and transfection

MEFs were used in the previous study [19, 20]. Briefly, cells were grown in Dulbecco's Modified Eagle's Medium (DMEM, Gibco-BRL, Grand Island, NY, USA) supplemented with 1% Glutamax, 1% MEM-NEAA, 10% FBS (Hyclone, south Logan, Itah, USA), 100 unit/ml penicillin, and 100 μg/ml streptomycin (Welgene, Seoul, Republic of Korea). Cells were maintained at 37 °C in a 5% CO_2 in a humidified incubator. For transfection, MEFs were electroporated with indicated plasmids using the Neon® transfection system (Thermo Fisher Scientific) according to manufacturer's instructions.

Generation of α-TAT1 KO cell line using CRISPR/Cas9

A 20-bp guide RNA (gRNA) sequence (5′-catggagttcccgttcgatg-3′), targeting genomic DNA within exon 1 of *Atat1,* was selected from a Genescript database of predicted high-specificity protospacer adjacent motif (PAM) sequence in the mouse exome. PX458 or PX458 containing gRNA and pLKO.1-puro (Addgene, #10878), were co-transfected into MEFs. Transfected cells were selected with puromycin (2 μg ml^{-1}) for 2 weeks, and single-cell colonies were acquired. α-TAT1 knockout in MEFs was verified by genomic DNA sequencing and western blotting.

Immunocytochemistry

Cells were seeded on fibronectin-coated 0.5 kPa PAG or glass 12-mm coverslips and incubated with or without TGF-β1 for 8 h. Samples were fixed with 3.7% paraformaldehyde for 15 min and permeabilized with 0.5% Triton X-100 in phosphate-buffered saline (PBS) for 10 min. To block non-specific signals, coverslips were blocked with 2% bovine serum albumin (BSA) in PBST (0.1% of Triton X-100 in PBS) for 1 h. Cells were then incubated with indicated primary antibodies (1:50 ~ 100) for 1 h, followed by incubation with the appropriate secondary antibodies for 1 h at room temperature (RT). Coverslips were mounted on glass slides with Fluoromount-G (Southern Biotechnology Associates, Birmingham, AL, USA) and analyzed using an Eclipse 80i fluorescence microscope (Nikon, Tokyo, Japan). Images were acquired using a digital camera (digital sightDS-Qi1Mc, Nikon) and NIS-Elements image analysis software (Nikon). Image processing was carried out using Photoshop 11.0 (Adobe Systems, San Jose, CA, USA).

Immunohistochemistry

Liver tissues were fixed with 4% paraformaldehyde and cryo-protected in increasing concentrations of sucrose solution (10, 20, and 30%) until tissue sinks. The tissues were then embedded in O.C.T compound (Tissue-Tek) and sectioned at 15 μm. The sections were blocked with M.O.M.™ blocking solution and normal goat serum (Vector Biolaboratories, Burlingame, CA, USA) for 1 h at RT. Tissues were then incubated with antibodies specific for α-SMA and Ac-α-tubulin. After removing the unbound primary antibody with PBS, the tissues were incubated with a secondary antibody in 2% normal goat serum at RT for 1 h. Afterwards, the tissues were washed in PBS and mounted with Fluoromount-G. Fluorescence-positive area was analyzed using imaging software NIS-Elements advanced research (Nikon).

Lentiviral production and infection

For virus production, HEK293T cells were co-transfected using lentiviral packaging plasmids (psPAX2 and pMD2.G) with a pLKO.1-blast plasmid (Addgene, Cambridge, MA, USA, #26655) containing shSmad2 or shYAP. After 24 h, the media were replaced with fresh media, and HEK293T were incubated for an additional 48 h. The media were collected and filtered using a 0.45 μm syringe filter. MEFs were treated with shRNA containing lentiviral particles with polybrene (final concentration 8 μg ml^{-1}) to enhance viral transduction. After 48 h, cells were selected using 5 μg ml^{-1} blasticidin (Sigma-Aldrich, #15205) in the growth medium. The oligonucleotide pairs used are listed as follows in Supplementary Table 1.

Protein isolation and Western blotting

Cells were lysed with lysis buffer containing 1% Nonidet P-40 (NP-40), 1% sodium dodecyl sulfate (SDS), 150 mM NaCl, 6 mM Na_2HPO_4, 4 mM NaH_2PO_4, 2 mM ethylenediaminetetraacetic acid (EDTA), 50 mM NaF, 1 mM Na_3VO_4, 1 mM 1,4-dithiothreitol (DTT), and 1 mM phenylmethylsulfonyl fluoride (PMSF). The membranes with bound proteins were incubated with the indicated primary antibodies for 12–16 h at 4 °C. Then, membranes were further incubated with horseradish peroxidase (HRP)-conjugated secondary antibodies (Jackson ImmunoResearch Laboratories, West Grove, PA, USA) for 1–2 h at RT. Signals were developed using enhanced chemiluminescence (Bio-Rad, Hercules, CA, USA) reagents, and band density was measured using a Quantity One® system (Bio-Rad).

Luciferase reporter assay

MEFs were transfected with 4 μg of 8xGTIIC-luciferase (Addgene, #34615), SBE2-luciferase (Addgene, #16500), and 4 μg of pCMV-β-galactosidase (Clontech Laboratories, Inc., CA, USA) using electroporation according to the manufacturer's protocol. After 24 h, the transfected

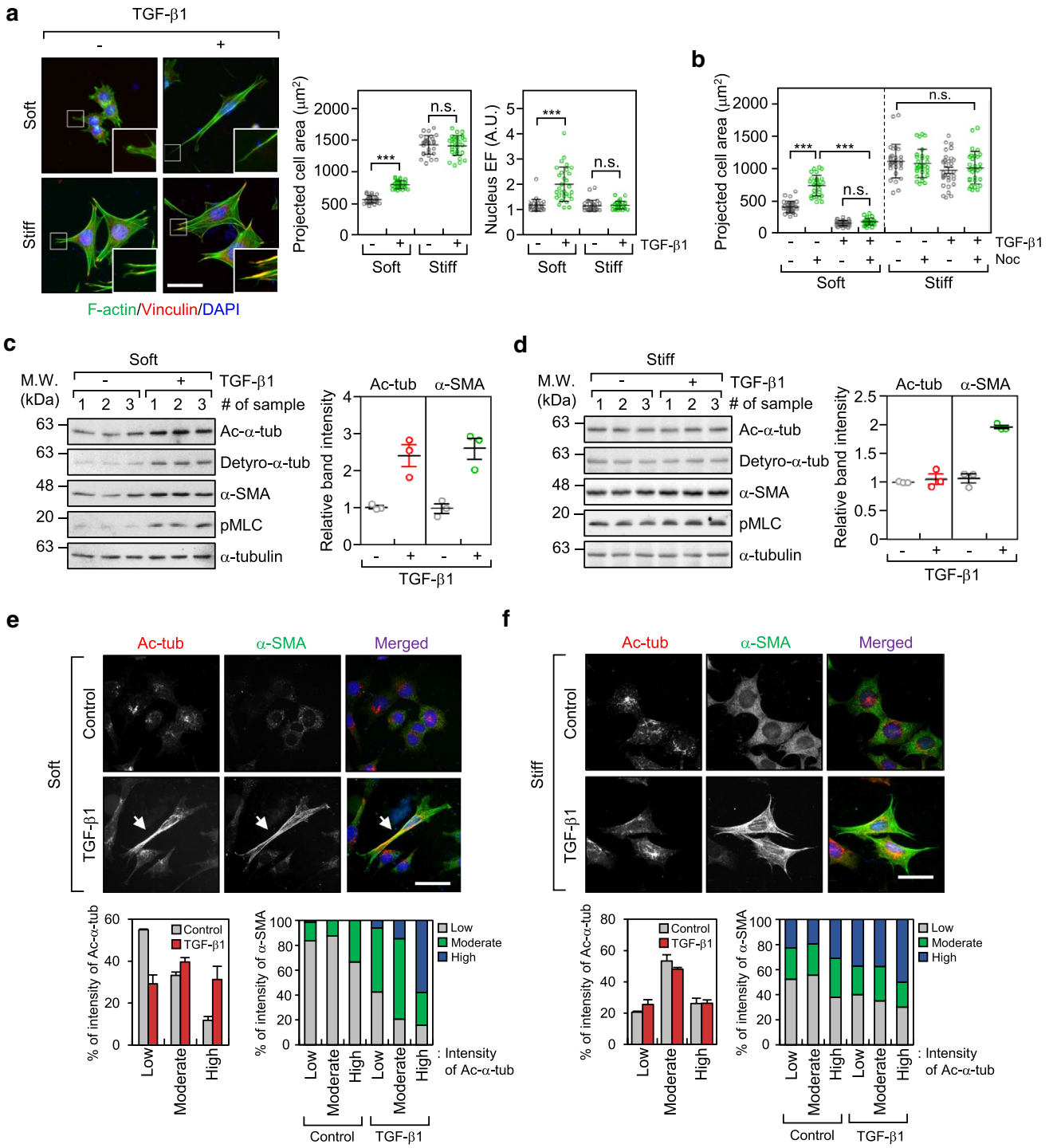

cells were serum-starved for 12 h and seeded on fibronectin-coated 0.5 kPa PAGs for 8 h with or without TGF-β1 (2 ng ml^{-1}). Cells were lysed using reporter lysis buffer (Promega, WI, USA), and lysates were analyzed using a GloMax® Luminometer (Promega). Transfection and expression efficiencies were normalized to the activity of β-galactosidase activities.

Quantitative real-time PCR

Total RNA was extracted using RNAiso Plus reagent (TaKaRa, Tokyo, Japan, #9109), and complementary DNA was synthesized using M-MLV reverse transcriptase (M. Biotech., Seoul, Republic of Korea). qPCR was conducted with SYBR Premix Ex-Taq II (Tli RNase H Plus, TaKaRa, #RR820A) per manufacturer's instructions on a

◂**Fig. 1** TGF-β1 increases microtubule acetylation on soft matrices. **a** Mouse embryonic fibroblasts (MEFs) were seeded on soft (0.5 kPa PAGs) and stiff (glass) conditions, stimulated with TGF-β1 (2 ng ml^{-1}) for 8 h, and then labelled using an antibody specific for vinculin and Alexa Fluor® 488 phalloidin. Data are represented as means ± S.D. from two independent experiments ($n = 30$). Statistical analysis was performed by one-way ANOVA with Tukey's multiple comparison test. ***$p < 0.005$, n.s. not significant. Projected cell area: one-way ANOVA, $F_{3, 116} = 423.8$, Nucleus EF: one-way ANOVA, $F_{3, 116} = 35.28$. Scale bar, 50 µm. **b** Comparison of projected cell area upon combinational treatment using TGF-β1 and/or nocodazole (Noc; 10 µM). Data are represented as means ± S.D. from two independent experiments ($n = 30$). Statistical analysis was performed by one-way ANOVA with Tukey's multiple comparison test. ***$p < 0.005$, n.s. not significant. One-way ANOVA, $F_{7, 232} = 138.6$. **c**, **d** Western blotting conducted to detect the level of post-translational modifications including acetylation and detyrosination, α-tubulin and α-SMA in TGF-β1-treated MEFs incubated on soft (**c**) and stiff (**d**) matrices. Protein lysates obtained from MEFs grown on soft and stiff, were prepared independently. Graph shows relative expression of α-tubulin acetylation and α-SMA normalized to the expression of α-tubulin. **e**, **f** Immunofluorescence labelling of acetylated-α-tubulin and α-SMA in MEFs incubated on soft (**e**) and stiff (**f**) matrices upon stimulation with TGF-β1. Expression of acetylated-α-tubulin and α-SMA was categorized using fluorescence intensity (low, moderate, and high). Graphs show the percentage of α-SMA expression as increasing fluorescence intensity of acetylated-α-tubulin. Arrows indicate co-expression of acetylated-α-tubulin and α-SMA in TGF-β1-treated MEFs grown under soft conditions. Scale bar, 50 µm

Quantstudio™3 instrument (Applied Biosystems) using primers listed in Supplementary Table 2. The expression level of each gene was calculated as $2^{-\Delta\Delta}$Ct and normalized to the Ct value of *Gapdh*. The results were obtained using three biological replicates and two or three technical replicates for each gene and sample.

Library preparation and RNA-sequencing

After total RNA was extracted from WT and α-TAT1 KO grown on soft matrix with or without TGF-β1, RNA quality was measured on an Agilent 2100 Bioanalyzer using an RNA 6000 Nano Chip (Agilent Technologies, Amstelveen, Netherlands). RNA quantification was performed using a ND-2000 Spectrophotometer. For control and test RNA, the construction of a library was performed using QuantSeq 3′ mRNA-Seq Library Prep Kit (Lexogen, Inc., Austria) according to the manufacturer's instructions. Each 500 ng of total RNA was prepared, then an oligo-dT primer containing an Illumina-compatible sequence at its 5′ end was hybridized to the RNA, and reverse transcription was conducted. After degradation of the RNA template, second-strand synthesis was initiated using a random primer containing an Illumina-compatible linker sequence at its 5′ end. The double-stranded library was purified using magnetic beads to remove all reaction components. The library was amplified to add the complete adapter sequences required for cluster generation. The finished library was purified from PCR components. High-throughput sequencing was performed as single-end 75 sequencing using NextSeq 500 (Illumina, Inc., USA).

Bioinformatic analysis

QuantSeq 3′ mRNA-Seq reads were aligned using Bowtie2. Bowtie2 indices were either generated from the genome assembly sequence or the representative transcript sequences for aligning to the genome and transcriptome. The alignment file was used for assembling transcripts, estimating their abundance and detecting differential expression of genes. Differentially expressed genes were determined based on counts from unique and multiple alignments using coverage in Bedtools. The Read Count data were processed based on the Global normalization method using the Genowiz™ version 4.0.5.6 (Ocimum Biosolutions, India). Hierarchical clustering analysis was performed using Pearson correlation as the distance metric. Functional classification of gene on searches done by PANTHER gene ontology (https://www.pantherdb.org). Survival rate in HCC patients was analyzed by Kaplan–Meier plot (https://kmplot.com).

Statistical analysis

Statistical analyses were performed in GraphPad Prism8 (GraphPad Software, California, USA). We used the one-way Analysis of Variance (ANOVA) for comparisons of more than two groups. Tukey's multiple comparison test was applied to all ANOVA analyses post-hoc test. ANOVA F values are depicted in each figure legend as $F_{(DFn, Dfd)}$, where DFn is the df nominator and Dfd the df denominator. p values of less than 0.05 were considered statistically significant. *$p < 0.05$, **$p < 0.01$, ***$p < 0.005$. All data are presented as means ± standard deviation (S.D.).

Results

Myofibroblast differentiation induced by TGF-β1 is accompanied by microtubule acetylation in cells grown on soft matrices

To compare the effects of TGF-β1 on myofibroblast differentiation with respect to substrate stiffness, MEFs were seeded on 0.5 kPa PAG substrates (soft) and glass coverslips (stiff) and cultured for 8 h with or without the presence of TGF-β1. As shown in Fig. 1a, TGF-β1 induced strong focal adhesions and formation of actin stress fibres in cells cultured on glass coverslips, but not in cells cultured on soft matrices. Formation of strong focal adhesions and actin stress fibres was nearly absent in cells cultured on soft PAG matrices. Instead, the prominent features of cells cultured on soft

PAG matrices included increased cell length, and increased ratio of nuclear length to width (represented by the nuclear elliptical factor [EF]) after treatment with TGF-β1 (Fig. 1a). Consistent with the results of previous studies, the spreading of fibroblasts on soft matrices [23], but not on stiff matrices, was completely inhibited by treatment with nocodazole, a microtubule disrupting agent (Fig. 1b). This result indicates that microtubules play an important role in the spreading of cells on soft matrices under TGF-β1 stimulation.

Previously, we reported that microtubule acetylation is critical for myofibroblast differentiation in SPIN90-depleted MEFs in a soft matrix environment [20]. In the present study, we confirmed that microtubule acetylation is also increased during myofibroblast differentiation induced by TGF-β1. Interestingly, acetylation and detyrosination of microtubule were significantly increased during myofibroblast differentiation induced by TGF-β1 on soft matrices, which was due to increased α-SMA expression (Fig. 1c; soft matrix). In contrast, those modifications did not induce by TGF-β under stiff substrate condition (Fig. 1d; stiff matrix). In addition to TGF-β1, LPA, another inducer of myofibroblast differentiation [24], increased the acetylation of microtubules and expression of α-SMA under soft substrate conditions (Supplementary Fig. 1a, b). Fibroblasts cultured on soft matrices show reduced integrin-mediated focal adhesion signalling [23, 25]. Therefore, we hypothesized that increased microtubule acetylation in fibroblasts cultured on a soft substrate is associated with the absence of integrin-mediated signalling. To test this hypothesis, we examined the extent of TGF-β1-induced microtubule acetylation after treatment with pharmacological inhibitors of integrin signalling in cells cultured on stiff. Fibroblasts treated with blebbistatin (myosin II inhibitor) and Y27632 (Rho-associated kinase inhibitor) showed an increase in microtubule acetylation induced by TGF-β1 even when cultured on a stiff substrate (Supplementary Fig. 2a, b). This result indicates that acetylated microtubules play a prominent role in myofibroblast differentiation under conditions of weak integrin signalling, such as when cultured on soft matrices and in a 3D environment.

To investigate the correlation between microtubule acetylation and expression of α-SMA, we examined its cellular localization in TGF-β1-treated MEFs cultured on soft and stiff matrices. The fluorescence intensities of α-SMA and acetylated-α-tubulin were arbitrarily divided into three categories; high, moderate, and low. Fibroblasts cultured on soft matrices exhibited high expression of α-SMA as the levels of acetylated-α-tubulin increased after stimulation with TGF-β1 (Fig. 1e). However, the relationship between acetylated-α-tubulin and α-SMA in fibroblasts cultured under stiff substrate conditions was unclear (Fig. 1f). We also found acetylated microtubules in cells cultured on soft substrates were distributed along the length of the cell, whereas in cells cultured on stiff substrates, they were present around the nucleus (Fig. 1e, f). These findings indicate that acetylated microtubules in the cell cultured under soft matrices are critical for cell spreading and morphogenesis.

Microtubule acetylation is required for TGF-β1-induced myofibroblast differentiation on soft matrices

To analyze the molecular mechanisms of microtubule acetylation in myofibroblast differentiation on soft substrates, we generated an MEF cell line in which the α-TAT1, encoded by *Atat1* gene was disrupted using the CRISPR/Cas9 system (α-TAT1 KO MEF; Fig. 2a, Supplementary Fig. 3a, b). We were unable to directly confirm the ablation of endogenous α-TAT1 protein expression in α-TAT1 KO MEFs via western blotting because there are no commercially available antibodies that bind the endogenous α-TAT1. However, two clones of the α-TAT1 KO MEF cell line were selected using DNA sequencing of the CRISPR/Cas9 target site in the *Atat1* gene and by the yield of tubulin acetylation (Fig. 2a). α-TAT1 KO MEFs showed a profound decrease in TGF-β-induced nuclear elongation (Fig. 2b). α-SMA (encoded by *Acta2* gene) transcription and protein expression were also inhibited in α-TAT1 KO MEFs cultured on soft substrates, while the level of detyrosinated tubulin, assessed under the same conditions, remained unchanged (Supplementary Fig. 3c, Fig. 2c). Cells incubated on a stiff substrate increased their expression of α-SMA in response to stimulation with TGF-β1 regardless of the presence of acetylated-α-tubulin (Fig. 2d). Fluorescence imaging confirmed that the expression of α-SMA induced by TGF-β occurred in α-TAT1 KO MEF, but was less than that in WT MEFs (Fig. 2e). Transient overexpression of GFP-α-TAT1 in WT MEFs increased the expression of α-SMA in response to stimulation with TGF-β (Fig. 2f), suggesting that acetylated microtubules are involved in TGF-β1-mediated myofibroblast differentiation on soft substrates.

We next investigated whether acetylated microtubules are required for fibroblast contractility and re-organization of 3D collagen matrix (Fig. 2g). Fibroblasts in floating matrix contraction (FMC) initially have a round morphology and then spread during contraction, which resembles cells in soft matrices. Fibroblasts in stressed matrix contraction (SMC) show a spread morphology with stress fibres and resemble the fibroblasts cultured on stiff substrates [9, 26]. As shown in Fig. 2h and i, α-TAT1 KO MEFs, stimulated with TGF-β1, did not increase the FMC, whereas both WT and α-TAT1 KO MEFs induced SMC to a similar extent in response to stimulation with TGF-β. This result indicates that acetylated microtubules play an important role in the contractility of cells grown on soft substrates before substrate develops tension.

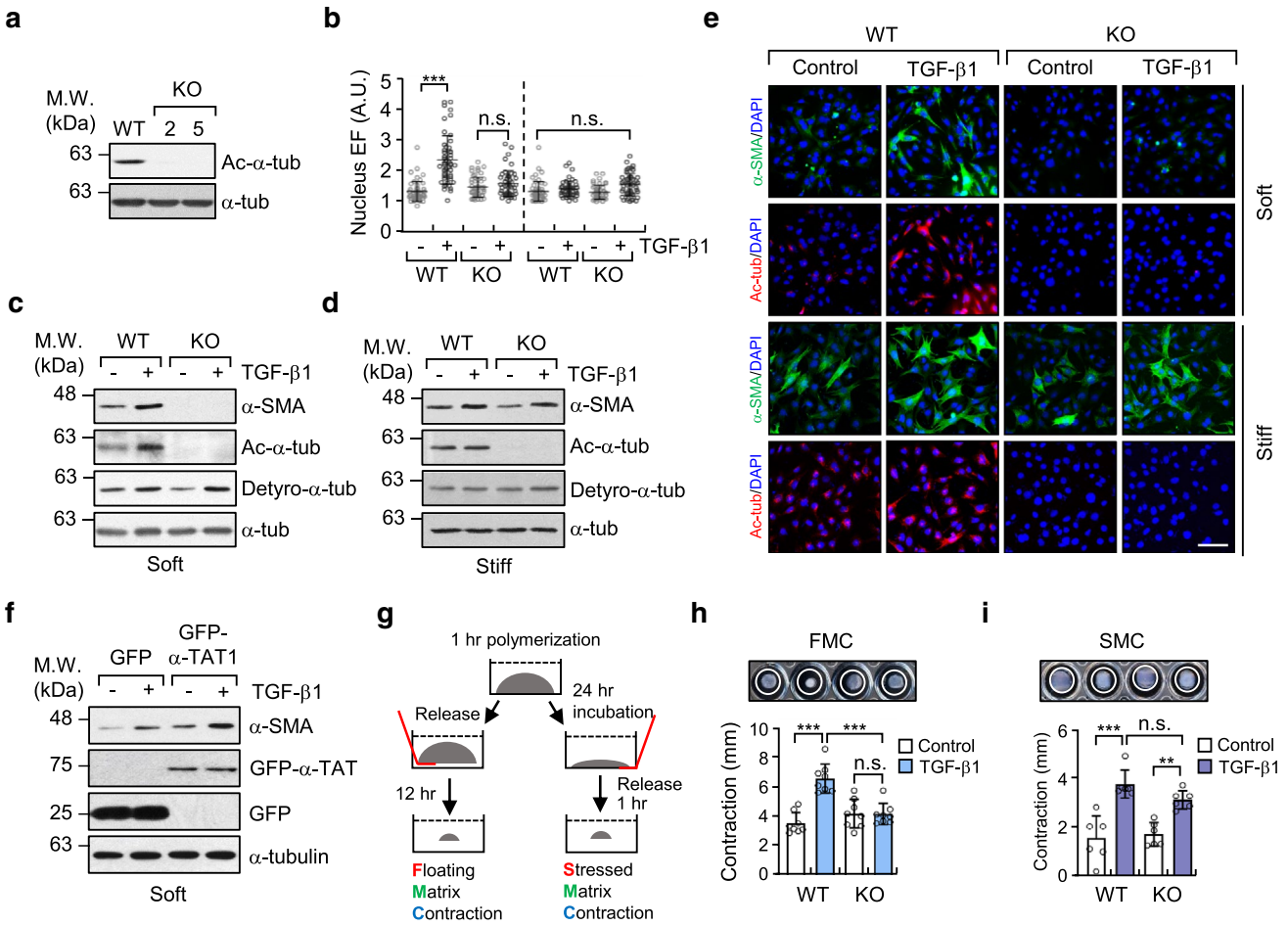

Fig. 2 Increase in microtubule acetylation is required for TGF-β1-induced myofibroblast differentiation on soft matrix**. a** Western blotting conducted to detect the level of acetylated-α-tubulin in α-TAT1 KO MEFs (clone #2 and 5) established using a CRISPR/Cas9 system. **b** Quantification of nuclear elliptical factor (EF) in WT and α-TAT1 KO MEFs upon treatment with TGF-β1 for 8 h. Data are represented as mean ± S.D. from two independent experiments ($n = 50$). Statistical analysis was performed by one-way ANOVA with Tukey's multiple comparisons. One-way ANOVA, $F_{7, 392} = 34.74$. **c**, **d** Western blotting of α-SMA in WT and α-TAT1 KO MEFs grown on soft (**c**) and stiff (**d**) matrices. **e** Immunofluorescence images of α-SMA (green) and acetylated-α-tubulin (red) in WT and α-TAT1 KO MEFs upon stimulation with TGF-β1. Scale bar, 100 μm. **f** MEFs were transfected with GFP or GFP-α-TAT1 for 24 h. After serum starvation for 12 h, cells were seeded on fibronectin-coated soft matrix and stimulated with TGF-β1 for 8 h. Cells were lysed and subjected to western blotting using antibodies specific for α-SMA and GFP. **g** Schematic diagram of 3D collagen matrix remodelling assays (FMC, floating matrix contraction; SMC, stressed matrix contraction). **h**, **i** WT and KO cells were embedded in 3D matrices composed of 1 mg ml^{-1} collagen and 100 μg ml^{-1} fibronectin, and incubated for 1 h. After adding TGF-β1 into each matrix, FMC (**h**) and SMC (**i**) assays were performed as shown in (**g**). Graphs show the reduced size of the 3D collagen gel compared with the original gel size. Data are represented as the mean of four independent experiments ± S.D. ($n = 8$, each group). FMC: one-way ANOVA, $F_{3, 28} = 19.59$, SMC: one-way ANOVA $F_{3, 20} = 17.91$. p value $p < 0.05$ considered being significant. $^{**}p < 0.01$, $^{***}p < 0.005$, n.s. not significant

Microtubule acetylation is involved in TGF-β1-induced expression of myofibroblast marker genes in MEFs grown on a soft substrate

To examine whether microtubule acetylation induces gene expression associated with myofibroblast differentiation in fibroblasts grown on a soft matrix, we performed RNA-sequencing analysis to compare the differentially expressed genes (DEGs) between WT and α-TAT1 KO MEFs seeded on a soft substrate in the absence or presence of TGF-β1 (Fig. 3a). The expression of 657 genes was significantly increased and that of 574 genes was significantly downregulated upon TGF-β1 stimulation (± 1.4-fold change, p value < 0.05; Fig. 3b, left). Among the 657 genes that were upregulated in WT MEFs upon stimulation with TGF-β1, 83 were downregulated in α-TAT1 KO MEFs (− 1.4-fold change, p-value < 0.05) (Fig. 3b, right). The biological process regulated by these 83 genes were assessed by gene ontology (GO) analysis (Fig. 3c). Of these 83 genes, 32 belonged to the top tier of genes for the

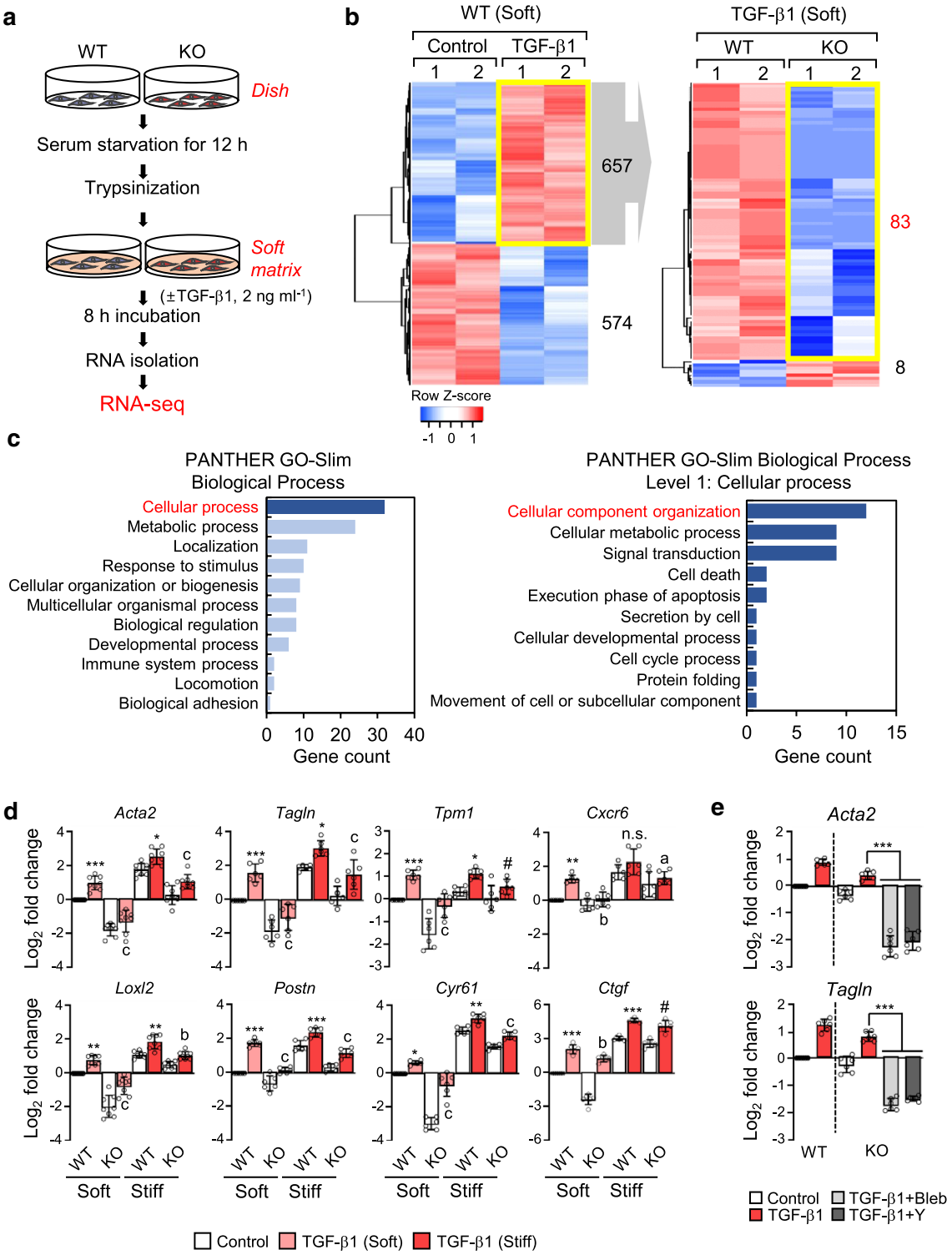

cellular process; the majority of these genes was involved in metabolic and cellular localization processes (Fig. 3c, left). We further investigated the specific functions of these genes involved in cellular processes and found that genes regulating the organization of cellular components, such as that of cytoskeletal binding proteins, appeared the highest level (Fig. 3c, right). During myofibroblast differentiation, cytoskeletal proteins play crucial roles in cell migration and contraction [27-29]; thus, genes whose expression is regulated by α-TAT1 are likely involved in cytoskeletal protein rearrangement and signal transduction during myofibroblast differentiation.

◂**Fig. 3** Differential gene expression in WT and α-TAT1 KO MEFs upon stimulation with TGF-β1. **a** Schematic diagram of the RNA-seq analysis workflow. **b** Left; Heatmap shows differentially expressed genes (DEGs; upregulated: 657, down-regulated: 574) in WT MEFs stimulated with TGF-β1. Right; DEGs between WT and KO upon TGF-β1 stimulation among 657 genes upregulated by TGF-β1. **c** Functional annotation of 83 genes selected on **b** (right) by PANTHER gene ontology. **d** Validation of myofibroblast marker genes using RT-qPCR. Data are represented as the mean of three independent experiments ± S.D. Statistical significance of the differences between the condition of TGF-β1 treated and untreated WT cells (control; $*p<0.05$, $**p<0.01$, $***p<0.005$, n.s. not significant) or the WT and KO cells in the condition of TGF-β1 treatment ($^{a}p<0.05$, $^{b}p<0.01$, $^{c}p<0.005$, # indicates not significant) was determined by one-way ANOVA with Tukey's multiple comparison. All comparisons between samples were performed within each condition of soft or stiff. One-way ANOVA, $F_{7,\ 56}=89.60$ (*Acta2*), $F_{7,\ 40}=48.92$ (*Tagln*), $F_{7,\ 40}=26.85$ (*Tpm1*), $F_{7,\ 40}=20.70$ (*Cxcr6*), $F_{7,\ 56}=87.53$ (*Loxl2*), $F_{7,\ 40}=97.13$ (*Postn*), $F_{7,\ 40}=246.7$ (*Cyr61*), $F_{7,\ 40}=286.3$ (*Ctgf*). **e** Transcript levels of *Acta2* and *Tagln* in α-TAT1 KO MEFs after combinational treatment with TGF-β1 and blebbistatin (Bleb)/or Y27632 (Y), incubated under stiff conditions. Data are represented the as mean ± S.D. from three independent experiments ($n=6$). Statistical significance of the differences between TGF-β1 treatment and TGF-β1 + blebbistatin or TGF-β1 + Y27632 treatment in α-TAT1 KO MEFs was determined by one-way ANOVA with Tukey's multiple comparisons. $***p<0.005$. *Acta2*: one-way ANOVA, $F_{5,\ 30}=178.6$, *Tagln*: one-way ANOVA, $F_{5,\ 30}=220$

Next, we determined the expression levels of 6 genes (*Acta2, Tagln, Tpm1, Cxcr6, Postn* and *Loxl2*) out of 83 genes associated with myofibroblast differentiation that were identified as upregulated genes in the WT cells treated with TGF-β1 compared with KO. In addition, because *Ctgf* and *Cyr61* genes were identified as significantly upregulated genes depending on microtubule acetylation [20], we also compared these genes expression by RT-qPCR analysis in soft and stiff conditions (Fig. 3d). RT-qPCR performed with samples obtained using cells cultured on soft matrices, showed that the 8 examined genes were upregulated by treatment with TGF-β1, whereas in α-TAT1 KO MEFs, treatment with TGF-β1 failed to induce the expression of these genes. Notably, differences in the gene expression induced by TGF-β1 in WT and α-TAT1 KO were not remarkable under stiff matrix conditions (Fig. 3d). In addition, treatment with blebbistatin and Y27632 dramatically inhibited the expression of *Acta2* and *Tagln*, decreasing it to basal levels in α-TAT1 KO MEFs under stiff matrix conditions (Fig. 3e). These results suggest that acetylated microtubules are indispensable for gene expression associated with myofibroblast differentiation in fibroblasts grown on a soft substrate.

Microtubule acetylation is required for YAP- and Smad-dependent transcriptional activity

We have previously reported that microtubule acetylation is associated with nuclear translocation of the YAP protein and induction of myofibroblast differentiation in MEFs grown on soft matrices [20]. In addition to YAP, the Smad transcription factor is also involved in the TGF-β-induced myofibroblast differentiation [30, 31]. Thus, we explored whether acetylated microtubules also regulate Smad activity in TGF-β-mediated myofibroblast differentiation under soft matrix conditions. MEF cell lines with a knockdown (KD) of YAP and Smad2 were established using shYAP and sh*S*mad2 viral vector expression. The expression of Smad and YAP in KD cells was knocked down by ~ 70% in transcript and protein levels (Fig. 4a). Analysis of myofibroblast marker gene expression upregulated by acetylation of microtubules showed that both Smad2 and YAP KD MEFs were inhibited to a similar extent in the expression of all tested genes, however, such as *Cxcr6*, *Cyr61* and *Ctgf* in Smad2 KD, and *Postn* in YAP KD did not show inhibited expression (Fig. 4b). Matrix contractility mediated by TGF-β1 was also significantly inhibited by the knockdown of Smad2 and YAP, respectively (Fig. 4c), indicating that contractile activity in Smad2 or YAP KD fibroblasts was similar to that in α-TAT1 KO fibroblasts.

To determine whether acetylated microtubules control the transcriptional activity of YAP and Smad in MEFs grown on a soft substrate, we performed a reporter assay for Smad and YAP using WT and α-TAT1 KO MEFs under soft and stiff matrix conditions (Fig. 4d, e). Interestingly, the transcriptional activity of Smad and YAP were dramatically reduced in α-TAT1 KO MEFs compared with that of WT MEFs stimulated with TGF-β1 under soft substrate conditions (Fig. 4d). Together, these findings indicate that acetylated microtubules are key regulators of TGF-β1-mediated YAP and Smad transcriptional activity in fibroblasts under soft substrate conditions but not under stiff substrate conditions.

YAP entered the nucleus via acetylated microtubule and increases Smad activity in soft substrate

The abovementioned results indicate that acetylated microtubules are required for YAP and Smad activities in soft substrate. Therefore, we next examined whether nuclear localization of phospho-Smad2/3 and YAP in cells grown on a soft substrate and stimulated with TGF-β1 is also regulated by acetylated microtubules. As shown in Fig. 5a, stimulation with TGF-β1 induced complete nuclear translocation of phospho-Smad2/3 in both WT and α-TAT1 KO MEFs. The amount of phospho-Smad2/3 in the nuclei of WT and α-TAT1 KO MEFs was similar. However, the less amount of nuclear YAP was detected in response to stimulation with TGF-β1 in α-TAT1 KO MEFs compared with those in WT MEFs under soft substrate conditions (Fig. 5a, Supplementary Fig. 4). Conversely, in cells grown on a stiff matrix, stimulation with TGF-β1 robustly induced the nuclear localization of phospho-Smad2/3 irrespective of the presence or absence of acetylated microtubule.

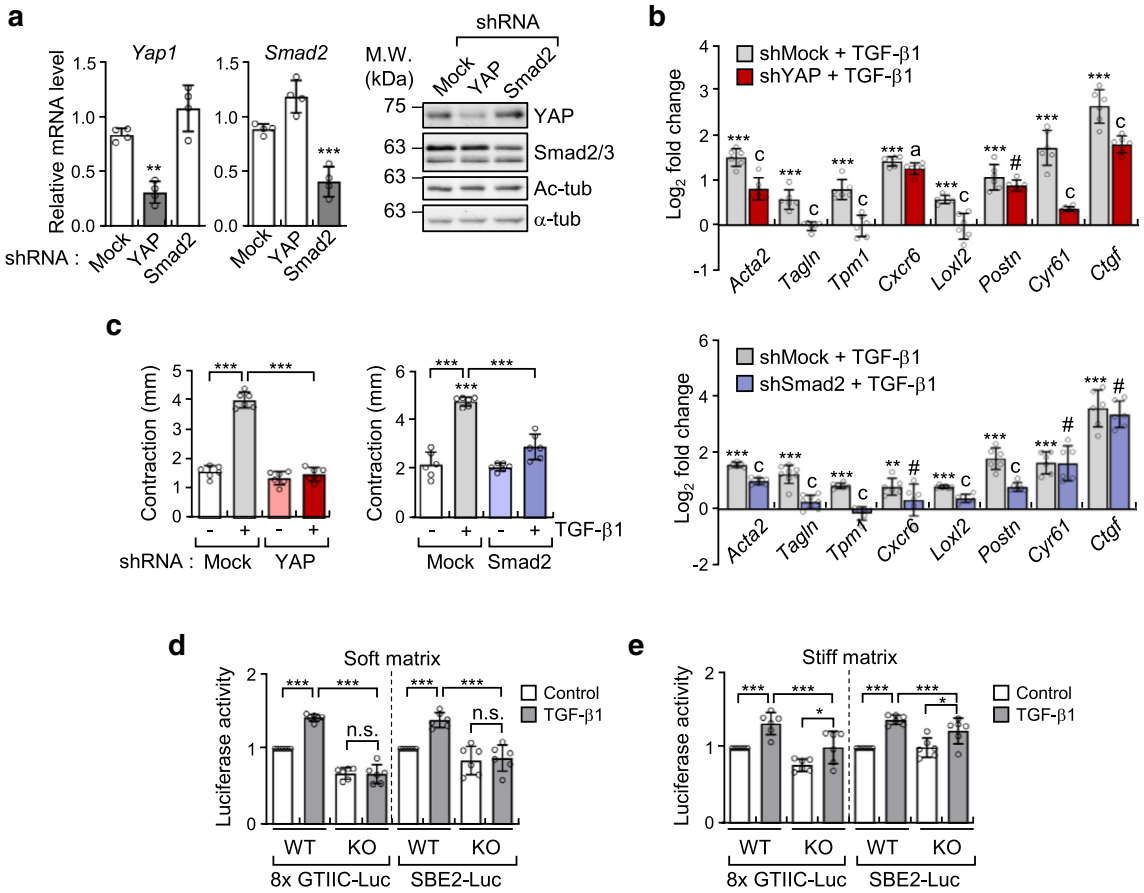

Fig. 4 Acetylation of microtubules induced by TGF-β1 regulates myofibroblast differentiation in YAP/Smad2-dependent manner. **a** Transcripts and protein levels of YAP and Smad2 in MEFs expressing pLKO.1-bla-shSmad2 and pLKO.1-bla-shYAP. Data are represented the mean of two independent experiments ± S.D. ($n = 4$). *Yap1*: one-way ANOVA, $F_{2,\ 9} = 31.93$, *Smad2*: one-way ANOVA, $F_{2,\ 9} = 43.41$. **b** RT-qPCR analysis conducted to compare gene expression in MEFs expressing pLKO.1-bla-shSmad2 and pLKO.1-bla-shYAP. Relative transcript level was normalized using pLKO.1-bla-transfected cells. Data are represented as mean ± S.D. from three independent experiments ($n = 6$). shYAP: one-way ANOVA, $F_{2,\ 15} = 102.9$ (*Acta2*), $F_{2,\ 15} = 36.21$ (*Tagln*), $F_{2,\ 15} = 37.34$ (*Tpm1*), $F_{2,\ 15} = 404.8$ (*Cxcr6*), $F_{2,\ 15} = 22.91$ (*Loxl2*), $F_{2,\ 15} = 63.34$ (*Postn*), $F_{2,\ 15} = 96.16$ (*Cyr61*), $F_{2,\ 15} = 186.6$ (*Ctgf*). shSmad2: one-way ANOVA, $F_{2,\ 15} = 514.7$ (*Acta2*), $F_{2,\ 21} = 63.72$ (*Tagln*), $F_{2,\ 15} = 76.62$ (*Tpm1*), $F_{2,\ 15} = 7.297$ (*Cxcr6*), $F_{2,\ 15} = 120.5$ (*Loxl2*), $F_{2,\ 15} = 84.94$ (*Postn*), $F_{2,\ 15} = 30.47$ (*Cyr61*), $F_{2,\ 15} = 109.6$ (*Ctgf*). **c** FMC assay conducted to evaluate the activity of pLKO.1-bla-shSmad2 and pLKO.1-bla-shYAP upon stimulation with TGF-β1. Graphs indicate reduced diameter of a 3D collagen gel compared with that of the original size. Data are represented as the mean of three independent experiments ± S.D. ($n = 6$). shYAP; one-way ANOVA, $F_{3,\ 20} = 178$, shSmad2; one-way ANOVA, $F_{3,\ 20} = 62.69$. **d**, **e** Luciferase reporter assay conducted to measure the transcriptional activity of YAP (8xGTIIC-Luc) and Smad (SBE2-Luc). WT and KO MEFs were transfected using SBE2-Luc or 8xGTIIC-Luc with CMV-β-galactosidase for 24 h. Cells were serum starved for 12 h, seeded on fibronectin-coated soft (**d**) or stiff matrices (**e**), and incubated for 8 h with TGF-β1. Luciferase activities were normalized using the activity of β-galactosidase. Data are represented as the mean of three independent experiments ± S.D. ($n = 6$). Soft; 8xGTIIC-Luc: one-way ANOVA $F_{3,\ 20} = 124.8$, SBE2-Luc: one-way ANOVA, $F_{3,\ 20} = 18.96$. Stiff; 8xGTIIC-Luc: one-way ANOVA, $F_{3,\ 20} = 16.36$, SBE2-Luc: one-way ANOVA, $F_{3,\ 20} = 16.14$. Statistical analysis was performed by one-way ANOVA with Tukey's multiple comparisons. p value $p < 0.05$ considered being significant. $^{*}p < 0.05$, $^{**}p < 0.01$, $^{***}p < 0.005$. For **b**, statistical significance between shMock and shYAP or shSmad2 under TGF-β1 stimulation was indicated with $^{a}p < 0.05$, $^{c}p < 0.005$, and #, not significant

Unstable phospho-Smad2/3 induce the de-phosphorylation and exported it out of the nucleus [32, 33]. Thus, it is possible that nuclear YAP translocated by acetylated microtubules, can maintain the phosphorylated status of Smad2/3 in the nucleus, thereby assisting the activity of Smad2/3 in the cell grown in soft substrates. As we expected, the knockdown of YAP significantly reduced the transcriptional activity of Smad2/3 induced by TGF-β1, while knockdown of Smad did not influence the transcriptional activity of YAP/TEAD (Fig. 5b, c). These findings are consistent with the results showing that inhibition of YAP with verteporfin, a pharmacological inhibitor, attenuates TGF-β1-induced nuclear accumulation of phospho-Smad, resulting in reduced expression of TGF-β1 target genes [33]. Overexpression of YAP active mutant (5SA) restored the transcriptional activity of Smad in α-TAT1 KO MEFs (Fig. 5d). Taken together,

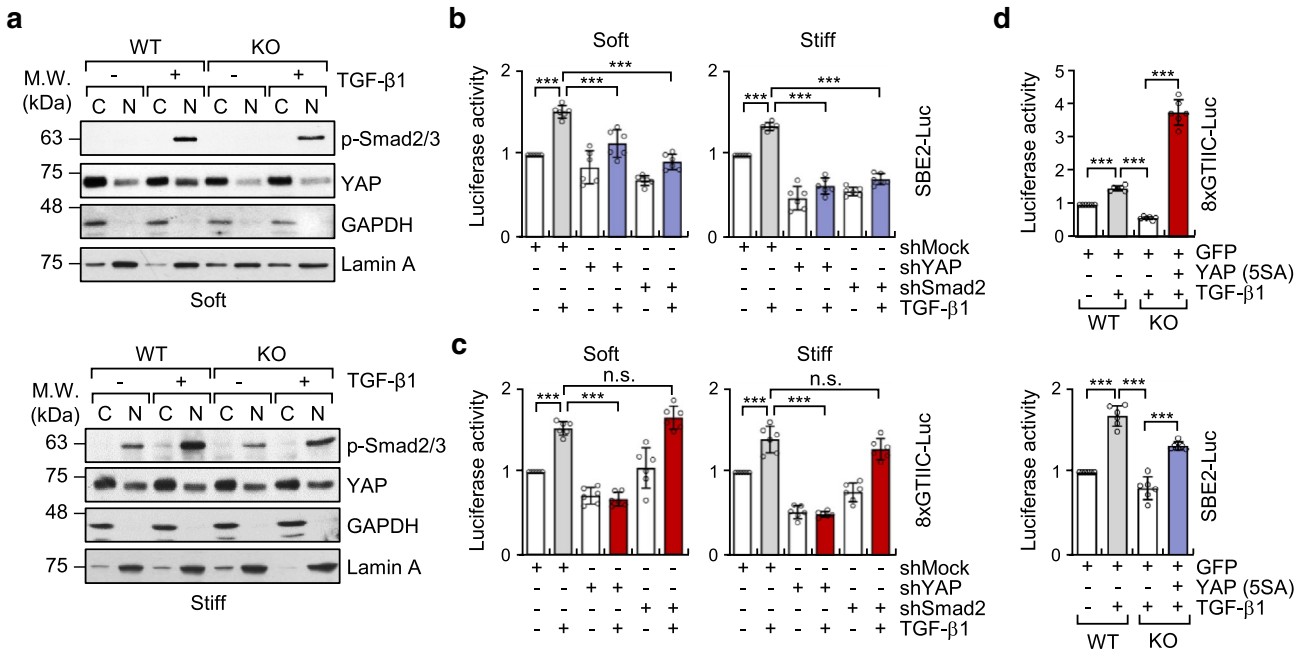

Fig. 5 Microtubule acetylation regulates TGF-β1-induced nuclear translocation of YAP, resulting in the promotion of Smad2 transcriptional activation**. a** Subcellular fractionation in WT and α-TAT1 KO MEFs incubated on soft and stiff matrices and stimulated with TGF-β1. Each fraction was used for western blotting with antibodies specific for phospho-Smad2/3 and YAP. GAPDH and Lamin A were used as markers for cytosolic and nucleic fraction, respectively. **b**, **c** Luciferase reporter assay for transcriptional activity of Smad (**b**; SBE2-Luc) and YAP (**c**; 8xGTIIC-Luc) in YAP and Smad2 KD cells incubated on soft or stiff matrices. Data are represented as mean of ± S.D. from three independent experiments ($n = 6$). SBE2-Luc: one-way ANOVA, $F_{5,30} = 35.25$ (soft), $F_{5,30} = 98.93$ (stiff). 8xGTIIC-Luc: one-way ANOVA, $F_{5,30} = 59.00$ (soft), $F_{5,30} = 85.86$ (stiff). **d** WT and α-TAT1 KO MEFs were transfected with the indicated plasmids (GFP or YAP(5SA)-GFP) for 24 h. WT and α-TAT1 KO MEFs were seeded on fibronectin-coated soft matrix and incubated for 8 h. Graphs show the relative luciferase activity of YAP and Smad. Data represent the mean of three independent experiments ± S.D. ($n = 6$). 8xGTIIC-Luc: one-way ANOVA, $F_{3,20} = 311.6$, SBE2-Luc: one-way ANOVA, $F_{3,20} = 95.15$. ***$p < 0.005$, n.s. not significant

these results support the hypothesis that nuclear translocation of YAP, induced by acetylated microtubules, promotes transcriptional activation of Smad2/3 in MEFs grown on soft matrices.

TGF-β1-induced YAP is translocated along with microtubule-dynein complex

Microtubule acetylation facilitates the accessibility of the motor proteins kinesin-1 and dynein to microtubules [34]. Increased accessibility of these motor proteins to acetylated microtubules promotes anterograde and retrograde transport of cargo proteins. Therefore, we examined whether the nuclear translocation of YAP by acetylated microtubules in a soft matrix is dependent on the motor protein dynein. To disturb dynein activity, WT MEFs were treated with pharmacological inhibitor of dynein, erythro-9-(2-hydroxy-3-nonyl) adenine (EHNA), which blocks ATPase and motor activity [35]. EHNA robustly inhibited TGF-β1-induced translocation of YAP into the nucleus without affecting cell morphology (Fig. 6a, b). Overexpression of dynamitin, which is reported to inhibit cytoplasmic dynein-based motility by inducing disassembly of dynactin [36], also dramatically inhibited TGF-β1-induced nuclear translocation of YAP on the soft substrate (Supplementary Fig. 5a, b). Conversely, the nuclear localization of phospho-Smad2/3 was not inhibited by EHNA, confirming the notion that nuclear translocation of phospho-Smad2/3 is independent of dynein activity (Fig. 6b). To further explore whether dynein indeed interacts with YAP via acetylated microtubule, we performed a microtubule sedimentation assay. When cells were treated with TGF-β1, YAP readily precipitated with dynein in WT, but not in α-TAT1 KO MEFs, indicating that YAP can form a tertiary complex with dynein and acetylated microtubules (Fig. 6c).

Next, we tested whether inhibition of dynein activity influences TGF-β1-induced transcriptional activity of YAP and Smad2/3. Treatment with EHNA dramatically suppressed the transcriptional activity of YAP/TEAD and Smad2/3, which was confirmed using reporter gene activity (Fig. 6d); however, treatment with EHNA did not change the amount of acetylated microtubules (Supplementary Fig. 6). Furthermore, the expression of myofibroblast marker genes, which are upregulated by TGF-β1 in MEFs grown

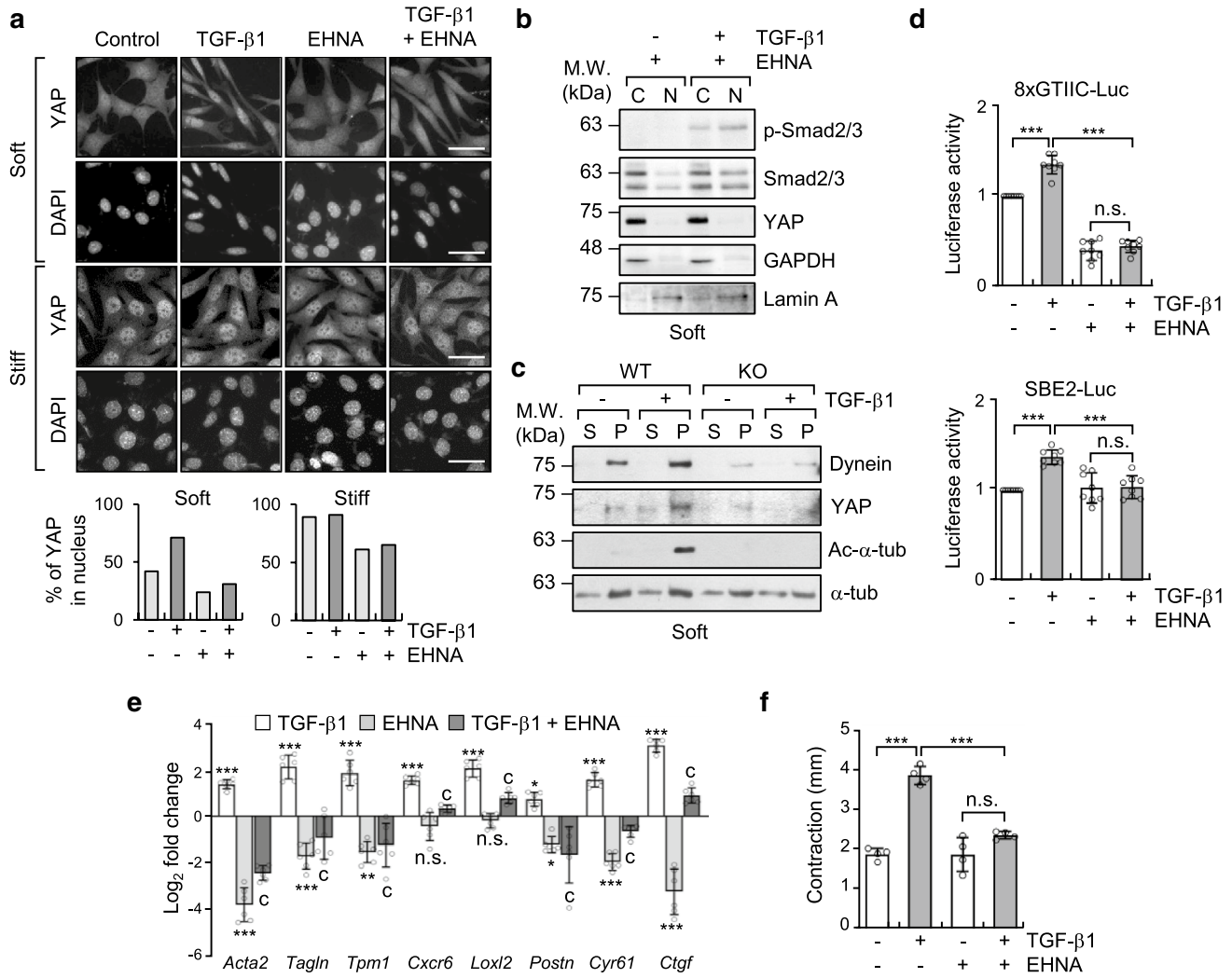

Fig. 6 Acetylated microtubules are sufficient for dynein-dependent nuclear translocation of YAP upon stimulation with TGF-β1. **a** Immunolabeling of YAP localization in WT and α-TAT1 KO MEFs treated with EHNA (500 μM) and/or TGF-β1 (2 ng ml^{-1}) and grown on fibronectin-coated soft and stiff matrices. Graphs show the percentage of YAP in the nucleus. Scale bar, 50 μm. **b** Western blotting analysis of nuclear and cytosolic fractions of WT MEFs treated with EHNA and/or TGF-β1 for 8 h. GAPDH and Lamin A were used as markers for cytosolic and nucleic fractions, respectively. **c** Microtubule sedimentation assay examining WT and α-TAT1 KO MEFs incubated on a soft matrix. Each fraction was assessed via western blotting to detect the levels of dynein and YAP. S; supernatant (depolymerized tubulin), P; pellet (polymerized tubulin). **d** Luciferase reporter assay in MEFs treated with TGF-β1 and EHNA and grown on 0.5 kPa PAGs. Data are represented as mean ± S.D. from three independent experiments ($n = 6$). 8xGTIIC-Luc: one-way ANOVA, $F_{3,\,28} = 246.9$, SBE2-Luc: one-way ANOVA, $F_{3,\,28} = 19.02$. $^{*}p < 0.05$, $^{**}p < 0.05$, $^{***}p < 0.005$, n.s. not significant. **e** RT-qPCR analysis of selected genes using the same conditions as those shown in **a**. Bar graph shows $\log_2$ fold change normalized to WT control. Data are represented as the mean of three independent experiments ± S.D. ($n = 6$). Statistical significance of the differences between each treatment and control group (baseline; $^{*}p < 0.05$, $^{**}p < 0.05$, $^{***}p < 0.005$, n.s., not significant) or between TGF-β1 treatment and EHNA + TGF-β1 ($^{c}p < 0.005$) was determined by one-way ANOVA with Tukey's multiple comparison. One-way ANOVA, $F_{3,\,20} = 201.5$ (*Acta2*), $F_{3,\,20} = 46.30$ (*Tagln*), $F_{3,\,20} = 41.05$ (*Tpm1*), $F_{3,\,20} = 41.29$ (*Cxcr6*), $F_{3,\,20} = 88.81$ (*Loxl2*), $F_{3,\,20} = 17.29$ (*Postn*), $F_{3,\,20} = 177.9$ (*Cyr61*), $F_{3,\,20} = 143.1$ (*Ctgf*). **f** WT MEFs were serum starved for 12 h and seeded into the collagen matrix. After 1 h, media containing TGF-β1 and/or EHNA were added into the matrices. Data are represented as the mean of two independent experiments ± S.D. ($n = 4$). One-way ANOVA, $F_{3,\,12} = 53.10$. $^{***}p < 0.005$, n.s. not significant

on a soft substrate, was significantly decreased by treatment with EHNA (Fig. 6e); therefore, 3D FMC was also greatly decreased (Fig. 6f).

It has reported that downregulation of Lissencephaly-1 (Lis1) as a part of dynein complex abrogates the dynein function [37]. We also found that knockdown of Lis1 in WT MEF significantly decreased the TGF-β1 induced transcriptional activity of YAP and Smad and cellular contractile ability upon TGF-β1 stimulation (Supplementary Fig. 7a–c). Altogether, these results indicate that dynein plays a critical

role in acetylated microtubule-mediated nuclear translocation of YAP upon stimulation with TGF-β1, which, in turn, initiates the myofibroblast differentiation along with Samd2/3 activity in MEFs grown on soft substrates.

Acetylated microtubules are critical for the progression of CCl_4-induced hepatic fibrosis

Our abovementioned results indicate that acetylated microtubules initiate myofibroblast differentiation in MEFs grown on a soft substrate. Based on this information, we next used a CCl_4-derived model of hepatic fibrosis to investigate whether acetylated microtubules appear in the early stage of fibrosis [38]. The administration of CCl_4 in mice causes liver damage and induces TGF-β1/Smad signaling, resulting in activation of hepatic stellate cells (HSCs) and fibroblasts [38, 39]. After mice were intraperitoneally (i.p.) injected with CCl_4 for 2 weeks, the amount of acetylated microtubule was remarkably increased in the liver tissue of CCl_4-treated mice compared with that in the livers of vehicle (corn oil)-treated mice; however, the expression of α-SMA was not significantly induced. As fibrosis progressed, the number of acetylated-α-tubulin positive cells was significantly increased, and these cells were dispersed in a radial arrangement (Fig. 7a). Notably, this CCl_4-induced increase in acetylated microtubules was abrogated by treatment with SB431542, a specific inhibitor of TGF-β receptor 1 (TβR1) (Fig. 7b). Western blotting, using samples shown in Fig. 7b, confirmed that the presence of acetylated microtubules and α-SMA expression, upregulated by CCl_4, were reduced in the mice treated with the SB431542, suggesting that TGF-β1 is a potent agonist that promotes the formation of acetylated microtubules in the early stage of liver fibrosis (Fig. 7c).

We next aimed to elucidate the relation between a set of genes regulated by acetylated microtubules and the expression of *Atat1* or *Hdac6* (which encode enzymes that catalyse α-tubulin deacetylation) in 40 liver cirrhosis patients (GSE25097). A significant positive correlation between *Atat1* and the target genes including *Acta2, Tpm1, Postn, Loxl2 and Cxcr6* was observed in the liver tissue (Supplementary Fig. 8a–g). In contrast, the mRNA expression level of these genes showed a reverse correlation with that of *Hdac6* (Supplementary Fig. 8a–g). Although *Ctgf* and *Cyr61* had high *p* values, these genes also showed the tendency of positive and reverse correlation with *Atat1* and *Hdac6* mRNA levels. The expression of *Yap1* was not correlated with those of *Atat1* and *Hdac6* (Supplementary Fig. 8h).

Finally, we compared the survival rate in patients with fibrotic disease according to the expression level of *Atat1*. Although we were not able to analyse the survival rate in patients with liver fibrosis, we analyzed the survival rate in high-risk hepatocellular carcinoma (HCC) patients ($n = 364$, probe ID; 79989 and 10013) using Kaplan–Meier plot. Patients with HCC also have liver cirrhosis, which develops after a long period of chronic liver disease [40]. Our results indicate clinical relevance between high levels of acetylated-microtubule and low survival rate in patient with HCC (Fig. 7d). Altogether, our findings demonstrate that TGF-β1 in an inflammatory environment induces fibrotic disease as a consequence of the promotion of microtubule acetylation. Our results suggest that targeting of acetylated-α-tubulin can be a novel therapeutic approach to overcome fibrotic disease.

Discussion

The increasing stiffness of normal stroma may provide a permissive environment for fibrotic disease. Myofibroblasts are the main cells that regulate the mechanical properties of tissue [13, 16]. Differentiation of fibroblasts into myofibroblasts has been studied extensively in association with fibrosis and wound healing. Studies examining myofibroblast differentiation in vitro indicate that myofibroblast differentiation requires a rigid ECM. However, one of the functions of myofibroblasts in vivo is to alter the stiffness of the ECM to render the tissue stiffer in pathological situations [41]; therefore, myofibroblast differentiation in vivo should initiate under conditions of soft ECM. Little is known about how myofibroblast differentiation occurs in an environment of mechanically soft ECM. In this study, we demonstrated that microtubule acetylation, induced by TGF-β1 is crucial for the expression of a set of myofibroblast marker genes. The expression of these genes regulated via YAP and Smad2/3 activity in soft matrices, initiates myofibroblast differentiation (Fig. 8).

The contractile force exerted by cells is increased by actomyosin activity after cells bind to ECM via activated integrin and focal adhesion structures [42]. When cells interact with mechanically stiff substrates, the activity of actomyosin and focal adhesions is increased by the Rho signalling pathway via activated integrin, resulting in increased tension and contractility of the cells. Conversely, in a soft environment such as normal tissue, a cell shows minimal integrin-dependent actomyosin activity; consequently, the contractile force exerted by the cell is relatively weak [9]. In a soft matrix, cells are placed in non-tensional state; therefore, gene expression is minimal. For this reason, cells must acquire specialized structures that are responsible for cell differentiation under conditions of soft ECM. The results of this study suggest that acetylated microtubules participate in regulating gene expression and myofibroblast differentiation under the condition of soft ECM. Our results, obtained using RNA-seq, reveal that acetylation of microtubules, induced by TGF-β1 under soft matrix conditions, increased the expression of

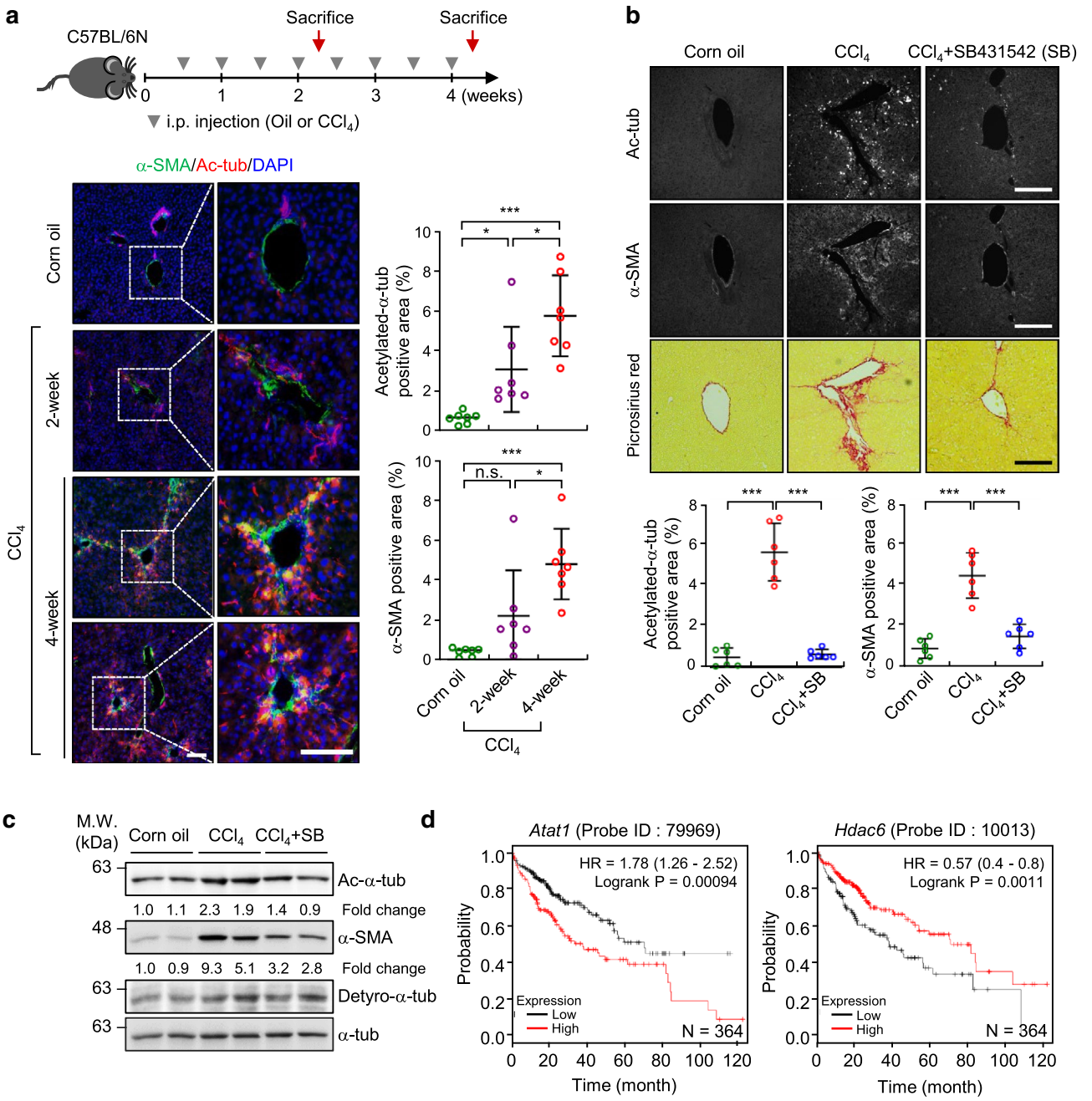

Fig. 7 Acetylation of α-tubulin is initiated during CCl_4-induced hepatic fibrosis. **a** Immunohistochemical (IHC) analysis of α-SMA and acetylated-α-tubulin expression in liver sections obtained from mice treated with corn oil or CCl_4 (0.5 ml kg^{-1} body weight, i.p., twice a week) for 2 and 4 weeks. Data are represented as the mean ± S.D. with $n = 7$ slices obtained from three mice per group. Acetylation of α-tubulin: one-way ANOVA, $F_{2,\ 18} = 15.74$, α-SMA: one-way ANOVA, $F_{2,\ 18} = 12.27$. Scale bar, 200 µm. **b** IHC analysis of α-SMA and acetylated-α-tubulin expression, and picrosirius red stain for thick-collagen expression, in liver sections of mice administered combined treatment with SB431542 and CCl_4 (10 mg kg^{-1} body weight, i.p., twice a week for 4 weeks). Data are represented as the mean ± S.D. with $n = 6$ slices obtained from three mice per group. Acetylation of α-tubulin: one-way ANOVA, $F_{2,\ 15} = 69.42$, α-SMA: one-way ANOVA, $F_{2,\ 15} = 36.29$. $^{*}p < 0.05$, $^{***}p < 0.005$, n.s. not significant. Scale bar, 200 µm. **c** Western blotting for detection of acetylated-α-tubulin, detyrosinated-α-tubulin and α-SMA in the liver sample obtained from **b**. **d** Survival analysis was conducted using Kaplan–Meier survival curves with respect to the expression level of *Atat1* (probe ID; 79969) and *Hdac6* (probe ID; 10013) in patients with hepatocellular carcinoma (HCC) ($n = 364$)

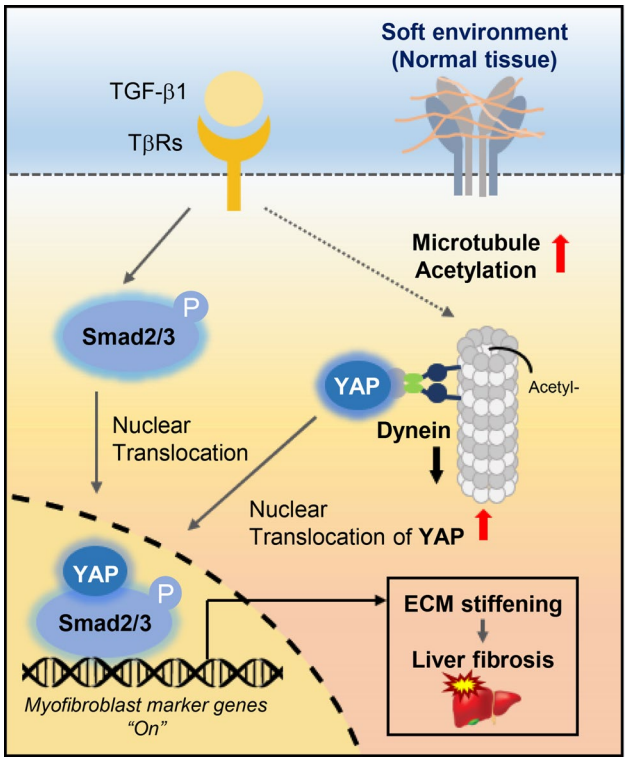

Fig. 8 Proposed model for TGF-β1-induced myofibroblast differentiation via microtubule acetylation on a soft matrix**.** Model showing entry of YAP into the nucleus through an acetylated microtubule and dynein complex accompanying the Smad2/3 complex in response to TGF-β1; this is required for myofibroblast differentiation on a soft matrix, which is critical for the progression of fibrotic diseases including liver fibrosis

approximately 83 genes that are involved in cytoskeletal reorganization and cellular processes. Among the genes, *Acta2*, *Tpm1* and *Tagln* are involved in cellular contractility [28, 43, 44]. We also found that the expression of *Loxl2*, encoding lysyl oxidase like-2 (LOXL2), which promotes ECM crosslinking and stabilization of the fibrotic matrix [45], is increased by acetylation of microtubules in soft matrices. Indeed, the *Loxl2* gene is significantly upregulated in fibrotic liver tissues [45]. Based on this evidence, it is possible that structural remodelling of ECM via upregulation of this gene by acetylated microtubule in early fibrotic tissues may generate a positive feedback loop. This loop would further induce the myofibroblast activation accompanied by intrinsic mechanotransduction signalling of YAP and myocardin-related transcription factor/serum response factor (MRTF/SRF) via Rho/ROCK-dependent cytoskeletal reorganization [15, 41, 46]. The expression of some of these genes, increased by acetylation of microtubules upon stimulation with TGF-β1, plays an important role in transforming the mechanical environment of soft tissue into a stiff environment during the process of fibrosis. Hence, acetylation of microtubules, induced by TGF-β1 in the soft environment, is an essential factor for controlling the mechanical properties of tissues.

Recent reports have shown that microtubule acetylation in MEFs is transiently increased by stimulation with TGF-β1. In MEFs and COS-7 cells, the carboxyl region of α-TAT1 acts as a regulatory domain in which TGF-β1-associated kinase1 (TAK1) can directly bind to, and phosphorylates, the Ser237 residue upon stimulation with TGF-β1; therefore, acetylation of microtubules is increased upon stimulation with TGF-β1 [47]. However, we were unable to induce microtubule acetylation with stimulation by TGF-β1 under stiff 2D conditions (Fig. 1d). This phenomenon has also been confirmed by other studies, showing that the amount of acetylated microtubules in cells such as fibroblasts, which originate from mesenchymal cells, is always upregulated regardless of the presence of growth factors when cells are under 2D stiff conditions [48]. Our results obviously show that the amount of acetylated microtubules is dramatically increased under soft matrix conditions and in the presence of growth factors involved in myofibroblast differentiation such as LPA or TGF-β1. According to the four-quadrant cell–matrix system [9], TGF-β1 signalling in soft ECM likely behaves differently than it does under stiff ECM conditions. TGF-β binds to the TGF-β receptor, which possesses serine/threonine kinase activity and controls the various intracellular signalling pathways [49]. As reported previously, the catalytic activity of α-TAT1 is controlled by phosphorylation of its relatively long c-terminal regulatory domain. Therefore, examining how downstream kinases of TGF-β1 receptor, such as extracellular signal-regulated kinase, p38 mitogen-activated protein kinase, and casein kinases [50] regulate α-TAT1 activity in soft substrate condition will help to develop new treatments against fibrotic disease.

In this study, we have shown that the nuclear translocation of YAP in response to stimulation with TGF-β1 is required for the formation of acetylated microtubule/dynein complex in soft substrates. Recent studies have reported that microtubule and actin cytoskeleton networks are required for the nuclear translocation of numerous virus- and cancer-related proteins [51, 52]. Microtubule binding protein p53 and PTH-related peptide (PTHrP) are translocated into the nucleus via interaction with importin β1 and importin α/β respectively [53, 54]. Heat shock protein 90 (Hsp90) also requires acetylated microtubule-based transport to enter the nucleus [52]. Fibroblast activation in the soft matrix is closely related to the characteristics of the microtubule network. Nuclear translocation of proteins in a microtubule-dependent manner is considered a major mechanism for the nuclear transport of proteins in a soft substrate. Interestingly, we also found that inhibition of dynein function by a pharmacological inhibitor or overexpression of dynamitin significantly reduced the nuclear translocation of the YAP protein, indicating that dynein plays a role in the nuclear

translocation of proteins. Some NLS-containing proteins can bind the dynein motor complex via interactions with dynein light chains. The NLS-containing protein then utilises the dynein motor complex to travel along the microtubules towards the nucleus [55]. Although YAP does not contain a canonical NLS, the N-terminal 1–55 amino acids of Yorkie (YAP homology in *Drosophila*), especially Arg-15, are essential for the nuclear localization of YAP via direct interaction with importin-α1 [56]. It is plausible that the interaction of YAP with microtubule/dynein complex in soft substrates leads to an accumulation of YAP in the nuclear periphery, where YAP containing non-canonical NLS is recognized by importin proteins.

Nevertheless, it is not clear how acetylated microtubules directly participate in the nuclear translocation of YAP in soft matrices. Recent studies have shown that the nuclear flattening, induced by ECM mechanical forces, is enough to initiate the nuclear translocation of YAP [57]. In a stiff matrix, YAP is translocated into the nucleus by ECM-nuclear mechanical coupling via linker of nucleoskeleton and cytoskeleton (LINC) complex. In our study, we observed changes in nuclear shape of MEFs stimulated with TGF-β1 under soft matrix conditions; these nuclear changes were inhibited by depletion of α-TAT1. In cells grown on a soft matrix, the nucleus is mechanically uncoupled from the ECM and is not exposed to external forces. In cells grown on a soft matrix and stimulated with TGF-β1, the increased tubulin acetylation results in altered nuclear shape, generating elongation (Fig. 1a, Fig. 2b). It is possible that tubulin acetylation provides mechanical support and dynein-dependent transport to cells stimulated with TGF-β1; this may constitute a mechanism for regulating YAP nuclear translocation after stimulation with TGF-β1 under soft matrix conditions. Therefore, our next challenge is to assess changes in the nuclear pore induced by acetylated microtubule in cells stimulated with TGF-β1.

The development of liver fibrosis is accompanied by progressive changes in the liver microenvironment. Liver fibrosis is strongly associated with excessive accumulation of ECM proteins, including collagen, resulting in cirrhosis, portal hypertension, and liver failure severe enough to require liver transplantation [58]. So far, anti-fibrotic therapies for the treatment of fibrotic diseases, including liver fibrosis and cirrhosis, have been extensively studied [59, 60]. As a result, drug development is underway to protect hepatocytes from damaged liver tissue induced by alcohol and reactive oxygen species (ROS) or to directly inhibit collagen synthesis, the activity of the ECM crosslinking enzyme, and the integrin/TGF-β1 signal [61-65]. For example, AB0023, an inhibitory antibody against LOXL2 was effective in a mouse model of liver fibrosis, where it reduced the number of activated fibroblasts and decreased the production of growth factors and cytokines [66]. Although this study suggests that inhibition of LOXL2 is a promising therapeutic target in fibrosis prevention or regression, clinical trials with the anti-LOXL2 antibody (simtuzumab) showed no anti-fibrotic effect in patients with hepatic fibrosis [60, 66-69]. This is probably due to the inability to restore the mechanical properties of the matrix of fibrotic tissues to those of the original tissue. Thus, it is important to find molecular markers to identify the early onset of fibrosis before changing the mechanical properties of this tissue and to prevent activation of the signaling pathway involved in tissue fibrosis. From this point of view, the results of our present study indicate that tubulin acetylation is a molecular marker for myofibroblast-derived pathogenesis in early fibrosis. Further, targeting of microtubule acetylation may be an effective strategy for the treatment of pathogenic conditions such as fibrosis.

Acknowledgements We are grateful to Prof. Young-Hwa Kim (Department of Applied Statistics, Chung-Ang University, Republic of Korea) for reviewing the statistical results. This research was supported by the National Research Foundation of Korea (NRF-2017R1A2B4004324) and the Korea Healthcare Technology R&D Project, Ministry for Health & Welfare Affairs (HI17C1620).

Author contributions EY and SR designed the project and wrote the manuscript. EY conducted the experiments. EY and SR analyzed the results. JJ and SK contributed to the experimental work. EY, PK and Y-JS contributed to the mouse experimental work. J-WK provided advice in the bioinformatic data. W-KS and SR supervised and administered the project, and all authors critically revised the manuscript and approved its final version.

Compliance with ethical standards

Conflict of interest The authors declare that they have no competing interests.

References

1. Engler AJ, Sen S, Sweeney HL, Discher DE (2006) Matrix elasticity directs stem cell lineage specification. Cell 126(4):677–689. https://doi.org/10.1016/j.cell.2006.06.044
2. Kim D, You E, Jeong J, Ko P, Kim JW, Rhee S (2017) DDR2 controls the epithelial-mesenchymal-transition-related gene expression via c-Myb acetylation upon matrix stiffening. Sci Rep 7(1):6847. https://doi.org/10.1038/s41598-017-07126-7
3. Joyce JA (2005) Therapeutic targeting of the tumor microenvironment. Cancer Cell 7(6):513–520. https://doi.org/10.1016/j.ccr.2005.05.024
4. Zou W (2005) Immunosuppressive networks in the tumour environment and their therapeutic relevance. Nat Rev Cancer 5(4):263–274. https://doi.org/10.1038/nrc1586
5. Provenzano PP, Inman DR, Eliceiri KW, Keely PJ (2009) Matrix density-induced mechanoregulation of breast cell phenotype, signaling and gene expression through a FAK-ERK linkage. Oncogene 28(49):4326–4343. https://doi.org/10.1038/onc.2009.299
6. Boutet A, De Frutos CA, Maxwell PH, Mayol MJ, Romero J, Nieto MA (2006) Snail activation disrupts tissue homeostasis and induces fibrosis in the adult kidney. EMBO J 25(23):5603–5613. https://doi.org/10.1038/sj.emboj.7601421

7. Hwang JH, Byun MR, Kim AR, Kim KM, Cho HJ, Lee YH, Kim J, Jeong MG, Hwang ES, Hong JH (2015) Extracellular matrix stiffness regulates osteogenic differentiation through MAPK activation. PLoS One 10(8):e0135519. https://doi.org/10.1371/journal.pone.0135519
8. Jeong J, Keum S, Kim D, You E, Ko P, Lee J, Kim J, Kim JW, Rhee S (2018) Spindle pole body component 25 homolog expressed by ECM stiffening is required for lung cancer cell proliferation. Biochem Biophys Res Commun 500(4):937–943. https://doi.org/10.1016/j.bbrc.2018.04.205
9. Rhee S, Grinnell F (2007) Fibroblast mechanics in 3D collagen matrices. Adv Drug Deliv Rev 59(13):1299–1305. https://doi.org/10.1016/j.addr.2007.08.006
10. Wang L, Qin W, Zhou Y, Chen B, Zhao X, Zhao H, Mi E, Mi E, Wang Q, Ning J (2017) Transforming growth factor beta plays an important role in enhancing wound healing by topical application of Povidone-iodine. Sci Rep 7(1):991. https://doi.org/10.1038/s41598-017-01116-5
11. Harris WT, Kelly DR, Zhou Y, Wang D, MacEwen M, Hagood JS, Clancy JP, Ambalavanan N, Sorscher EJ (2013) Myofibroblast differentiation and enhanced TGF-B signaling in cystic fibrosis lung disease. PLoS One 8(8):e70196. https://doi.org/10.1371/journal.pone.0070196
12. Hardie WD, Glasser SW, Hagood JS (2009) Emerging concepts in the pathogenesis of lung fibrosis. Am J Pathol 175(1):3–16. https://doi.org/10.2353/ajpath.2009.081170
13. Hinz B (2007) Formation and function of the myofibroblast during tissue repair. J Invest Dermatol 127(3):526–537. https://doi.org/10.1038/sj.jid.5700613
14. Tomasek JJ, Gabbiani G, Hinz B, Chaponnier C, Brown RA (2002) Myofibroblasts and mechano-regulation of connective tissue remodelling. Nat Rev Mol Cell Biol 3(5):349–363. https://doi.org/10.1038/nrm809
15. Calvo F, Ege N, Grande-Garcia A, Hooper S, Jenkins RP, Chaudhry SI, Harrington K, Williamson P, Moeendarbary E, Charras G, Sahai E (2013) Mechanotransduction and YAP-dependent matrix remodelling is required for the generation and maintenance of cancer-associated fibroblasts. Nat Cell Biol 15(6):637–646. https://doi.org/10.1038/ncb2756
16. Gabbiani G (2003) The myofibroblast in wound healing and fibrocontractive diseases. J Pathol 200(4):500–503. https://doi.org/10.1002/path.1427
17. Hinz B, Phan SH, Thannickal VJ, Galli A, Bochaton-Piallat ML, Gabbiani G (2007) The myofibroblast: one function, multiple origins. Am J Pathol 170(6):1807–1816. https://doi.org/10.2353/ajpath.2007.070112
18. Huang X, Yang N, Fiore VF, Barker TH, Sun Y, Morris SW, Ding Q, Thannickal VJ, Zhou Y (2012) Matrix stiffness-induced myofibroblast differentiation is mediated by intrinsic mechanotransduction. Am J Respir Cell Mol Biol 47(3):340–348. https://doi.org/10.1165/rcmb.2012-0050OC
19. You E, Huh YH, Lee J, Ko P, Jeong J, Keum S, Kim J, Kwon A, Song WK, Rhee S (2019) Downregulation of SPIN90 promotes fibroblast activation via periostin-FAK-ROCK signaling module. J Cell Physiol 234(6):9216–9224. https://doi.org/10.1002/jcp.27600
20. You E, Huh YH, Kwon A, Kim SH, Chae IH, Lee OJ, Ryu JH, Park MH, Kim GE, Lee JS, Lee KH, Lee YS, Kim JW, Rhee S, Song WK (2017) SPIN90 depletion and microtubule acetylation mediate stromal fibroblast activation in breast cancer progression. Cancer Res 77(17):4710–4722. https://doi.org/10.1158/0008-5472.CAN-17-0657
21. Maller O, DuFort CC, Weaver VM (2013) YAP forces fibroblasts to feel the tension. Nat Cell Biol 15(6):570–572. https://doi.org/10.1038/ncb2777
22. Piersma B, de Rond S, Werker PM, Boo S, Hinz B, van Beuge MM, Bank RA (2015) YAP1 is a driver of myofibroblast differentiation in normal and diseased fibroblasts. Am J Pathol 185(12):3326–3337. https://doi.org/10.1016/j.ajpath.2015.08.011
23. Rhee S, Jiang H, Ho CH, Grinnell F (2007) Microtubule function in fibroblast spreading is modulated according to the tension state of cell-matrix interactions. Proc Natl Acad Sci USsA 104(13):5425–5430. https://doi.org/10.1073/pnas.0608030104
24. Mazzocca A, Dituri F, Lupo L, Quaranta M, Antonaci S, Giannelli G (2011) Tumor-secreted lysophostatidic acid accelerates hepatocellular carcinoma progression by promoting differentiation of peritumoral fibroblasts in myofibroblasts. Hepatology 54(3):920–930. https://doi.org/10.1002/hep.24485
25. Mih JD, Marinkovic A, Liu F, Sharif AS, Tschumperlin DJ (2012) Matrix stiffness reverses the effect of actomyosin tension on cell proliferation. J Cell Sci 125(Pt 24):5974–5983. https://doi.org/10.1242/jcs.108886
26. Grinnell F, Ho CH, Lin YC, Skuta G (1999) Differences in the regulation of fibroblast contraction of floating versus stressed collagen matrices. J Biol Chem 274(2):918–923
27. Cai GQ, Chou CF, Hu M, Zheng A, Reichardt LF, Guan JL, Fang H, Luckhardt TR, Zhou Y, Thannickal VJ, Ding Q (2012) Neuronal Wiskott-Aldrich syndrome protein (N-WASP) is critical for formation of alpha-smooth muscle actin filaments during myofibroblast differentiation. Am J Physiol Lung Cell Mol Physiol 303(8):L692–702. https://doi.org/10.1152/ajplung.00390.2011
28. Gimona M, Sparrow MP, Strasser P, Herzog M, Small JV (1992) Calponin and SM 22 isoforms in avian and mammalian smooth muscle. Absence of phosphorylation in vivo. Eur J Biochem 205(3):1067–1075
29. Rockey DC, Weymouth N, Shi Z (2013) Smooth muscle alpha actin (Acta 2) and myofibroblast function during hepatic wound healing. PLoS One 8(10):e77166. https://doi.org/10.1371/journal.pone.0077166
30. de Caestecker MP, Parks WT, Frank CJ, Castagnino P, Bottaro DP, Roberts AB, Lechleider RJ (1998) Smad2 transduces common signals from receptor serine-threonine and tyrosine kinases. Genes Dev 12(11):1587–1592
31. Nakao A, Imamura T, Souchelnytskyi S, Kawabata M, Ishisaki A, Oeda E, Tamaki K, Hanai J, Heldin CH, Miyazono K, ten Dijke P (1997) TGF-beta receptor-mediated signalling through Smad2, Smad3 and Smad4. EMBO J 16(17):5353–5362. https://doi.org/10.1093/emboj/16.17.5353
32. Lin X, Duan X, Liang YY, Su Y, Wrighton KH, Long J, Hu M, Davis CM, Wang J, Brunicardi FC, Shi Y, Chen YG, Meng A, Feng XH (2006) PPM1A functions as a Smad phosphatase to terminate TGFbeta signaling. Cell 125(5):915–928. https://doi.org/10.1016/j.cell.2006.03.044
33. Szeto SG, Narimatsu M, Lu M, He X, Sidiqi AM, Tolosa MF, Chan L, De Freitas K, Bialik JF, Majumder S, Boo S, Hinz B, Dan Q, Advani A, John R, Wrana JL, Kapus A, Yuen DA (2016) YAP/TAZ are mechanoregulators of TGF-beta-Smad signaling and renal fibrogenesis. J Am Soc Nephrol 27(10):3117–3128. https://doi.org/10.1681/ASN.2015050499
34. Reed NA, Cai D, Blasius TL, Jih GT, Meyhofer E, Gaertig J, Verhey KJ (2006) Microtubule acetylation promotes kinesin-1 binding and transport. Curr Biol 16(21):2166–2172. https://doi.org/10.1016/j.cub.2006.09.014
35. Lin J, Nicastro D (2018) Asymmetric distribution and spatial switching of dynein activity generates ciliary motility. Science. https://doi.org/10.1126/science.aar1968
36. Burkhardt JK, Echeverri CJ, Nilsson T, Vallee RB (1997) Overexpression of the dynamitin (p50) subunit of the dynactin complex disrupts dynein-dependent maintenance of membrane organelle distribution. J Cell Biol 139(2):469–484
37. Baumbach J, Murthy A, McClintock MA, Dix CI, Zalyte R, Hoang HT, Bullock SL (2017) Lissencephaly-1 is a

context-dependent regulator of the human dynein complex. Elife. https://doi.org/10.7554/eLife.21768
38. Han CY, Koo JH, Kim SH, Gardenghi S, Rivella S, Strnad P, Hwang SJ, Kim SG (2016) Hepcidin inhibits Smad3 phosphorylation in hepatic stellate cells by impeding ferroportin-mediated regulation of Akt. Nat Commun 7:13817. https://doi.org/10.1038/ncomms13817
39. Yin C, Evason KJ, Asahina K, Stainier DY (2013) Hepatic stellate cells in liver development, regeneration, and cancer. J Clin Invest 123(5):1902–1910. https://doi.org/10.1172/JCI66369
40. Fattovich G, Stroffolini T, Zagni I, Donato F (2004) Hepatocellular carcinoma in cirrhosis: incidence and risk factors. Gastroenterology 127(5 Suppl 1):S35–50
41. Liu F, Lagares D, Choi KM, Stopfer L, Marinkovic A, Vrbanac V, Probst CK, Hiemer SE, Sisson TH, Horowitz JC, Rosas IO, Fredenburgh LE, Feghali-Bostwick C, Varelas X, Tager AM, Tschumperlin DJ (2015) Mechanosignaling through YAP and TAZ drives fibroblast activation and fibrosis. Am J Physiol Lung Cell Mol Physiol 308(4):L344–357. https://doi.org/10.1152/ajplung.00300.2014
42. Chan MW, Chaudary F, Lee W, Copeland JW, McCulloch CA (2010) Force-induced myofibroblast differentiation through collagen receptors is dependent on mammalian diaphanous (mDia). J Biol Chem 285(12):9273–9281. https://doi.org/10.1074/jbc.M109.075218
43. Hinz B, Celetta G, Tomasek JJ, Gabbiani G, Chaponnier C (2001) Alpha-smooth muscle actin expression upregulates fibroblast contractile activity. Mol Biol Cell 12(9):2730–2741. https://doi.org/10.1091/mbc.12.9.2730
44. Schevzov G, Lloyd C, Hailstones D, Gunning P (1993) Differential regulation of tropomyosin isoform organization and gene expression in response to altered actin gene expression. J Cell Biol 121(4):811–821
45. Wong CC, Tse AP, Huang YP, Zhu YT, Chiu DK, Lai RK, Au SL, Kai AK, Lee JM, Wei LL, Tsang FH, Lo RC, Shi J, Zheng YP, Wong CM, Ng IO (2014) Lysyl oxidase-like 2 is critical to tumor microenvironment and metastatic niche formation in hepatocellular carcinoma. Hepatology 60(5):1645–1658. https://doi.org/10.1002/hep.27320
46. Esnault C, Stewart A, Gualdrini F, East P, Horswell S, Matthews N, Treisman R (2014) Rho-actin signaling to the MRTF coactivators dominates the immediate transcriptional response to serum in fibroblasts. Genes Dev 28(9):943–958. https://doi.org/10.1101/gad.239327.114
47. Shah N, Kumar S, Zaman N, Pan CC, Bloodworth JC, Lei W, Streicher JM, Hempel N, Mythreye K, Lee NY (2018) TAK1 activation of alpha-TAT1 and microtubule hyperacetylation control AKT signaling and cell growth. Nat Commun 9(1):1696. https://doi.org/10.1038/s41467-018-04121-y
48. Gu S, Liu Y, Zhu B, Ding K, Yao TP, Chen F, Zhan L, Xu P, Ehrlich M, Liang T, Lin X, Feng XH (2016) Loss of alpha-tubulin acetylation is associated with TGF-beta-induced epithelial-mesenchymal transition. J Biol Chem 291(10):5396–5405. https://doi.org/10.1074/jbc.M115.713123
49. Derynck R, Zhang YE (2003) Smad-dependent and Smad-independent pathways in TGF-beta family signalling. Nature 425(6958):577–584. https://doi.org/10.1038/nature02006
50. Kim J, Hwan Kim S (2013) CK2 inhibitor CX-4945 blocks TGF-beta1-induced epithelial-to-mesenchymal transition in A549 human lung adenocarcinoma cells. PLoS One 8(9):e74342. https://doi.org/10.1371/journal.pone.0074342
51. Bremner KH, Scherer J, Yi J, Vershinin M, Gross SP, Vallee RB (2009) Adenovirus transport via direct interaction of cytoplasmic dynein with the viral capsid hexon subunit. Cell Host Microbe 6(6):523–535. https://doi.org/10.1016/j.chom.2009.11.006
52. Giustiniani J, Daire V, Cantaloube I, Durand G, Pous C, Perdiz D, Baillet A (2009) Tubulin acetylation favors Hsp90 recruitment to microtubules and stimulates the signaling function of the Hsp90 clients Akt/PKB and p53. Cell Signal 21(4):529–539. https://doi.org/10.1016/j.cellsig.2008.12.004
53. Lam MH, Briggs LJ, Hu W, Martin TJ, Gillespie MT, Jans DA (1999) Importin beta recognizes parathyroid hormone-related protein with high affinity and mediates its nuclear import in the absence of importin alpha. J Biol Chem 274(11):7391–7398
54. Roth DM, Moseley GW, Glover D, Pouton CW, Jans DA (2007) A microtubule-facilitated nuclear import pathway for cancer regulatory proteins. Traffic 8(6):673–686. https://doi.org/10.1111/j.1600-0854.2007.00564.x
55. Wagstaff KM, Jans DA (2009) Importins and beyond: non-conventional nuclear transport mechanisms. Traffic 10(9):1188–1198. https://doi.org/10.1111/j.1600-0854.2009.00937.x
56. Wang S, Lu Y, Yin MX, Wang C, Wu W, Li J, Wu W, Ge L, Hu L, Zhao Y, Zhang L (2016) Importin alpha1 mediates yorkie nuclear import via an N-terminal non-canonical nuclear localization signal. J Biol Chem 291(15):7926–7937. https://doi.org/10.1074/jbc.M115.700823
57. Elosegui-Artola A, Andreu I, Beedle AEM, Lezamiz A, Uroz M, Kosmalska AJ, Oria R, Kechagia JZ, Rico-Lastres P, Le Roux AL, Shanahan CM, Trepat X, Navajas D, Garcia-Manyes S, Roca-Cusachs P (1410e) Force triggers YAP nuclear entry by regulating transport across nuclear pores. Cell 171(6):1397–1410e1314. https://doi.org/10.1016/j.cell.2017.10.008
58. Bataller R, Brenner DA (2005) Liver fibrosis. J Clin Invest 115(2):209–218. https://doi.org/10.1172/JCI24282
59. Schuppan D, Ashfaq-Khan M, Yang AT, Kim YO (2018) Liver fibrosis: direct antifibrotic agents and targeted therapies. Matrix Biol 68–69:435–451. https://doi.org/10.1016/j.matbio.2018.04.006
60. Weiskirchen R, Weiskirchen S, Tacke F (2018) Recent advances in understanding liver fibrosis: bridging basic science and individualized treatment concepts. Res. 10.12688/f1000research.14841.1.
61. Reed NI, Jo H, Chen C, Tsujino K, Arnold TD, DeGrado WF, Sheppard D (2015) The alphavbeta1 integrin plays a critical in vivo role in tissue fibrosis. Sci Transl Med 7(288):288ra279. https://doi.org/10.1126/scitranslmed.aaa5094
62. Jimenez Calvente C, Sehgal A, Popov Y, Kim YO, Zevallos V, Sahin U, Diken M, Schuppan D (2015) Specific hepatic delivery of procollagen alpha1(I) small interfering RNA in lipid-like nanoparticles resolves liver fibrosis. Hepatology 62(4):1285–1297. https://doi.org/10.1002/hep.27936
63. Henderson NC, Arnold TD, Katamura Y, Giacomini MM, Rodriguez JD, McCarty JH, Pellicoro A, Raschperger E, Betsholtz C, Ruminski PG, Griggs DW, Prinsen MJ, Maher JJ, Iredale JP, Lacy-Hulbert A, Adams RH, Sheppard D (2013) Targeting of alphav integrin identifies a core molecular pathway that regulates fibrosis in several organs. Nat Med 19(12):1617–1624. https://doi.org/10.1038/nm.3282
64. Sugiyama A, Kanno K, Nishimichi N, Ohta S, Ono J, Conway SJ, Izuhara K, Yokosaki Y, Tazuma S (2016) Periostin promotes hepatic fibrosis in mice by modulating hepatic stellate cell activation via alphav integrin interaction. J Gastroenterol 51(12):1161–1174. https://doi.org/10.1007/s00535-016-1206-0
65. Weiskirchen R (2015) Hepatoprotective and anti-fibrotic agents: it's time to take the next step. Front Pharmacol 6:303. https://doi.org/10.3389/fphar.2015.00303
66. Barry-Hamilton V, Spangler R, Marshall D, McCauley S, Rodriguez HM, Oyasu M, Mikels A, Vaysberg M, Ghermazien H, Wai C, Garcia CA, Velayo AC, Jorgensen B, Biermann D, Tsai D, Green J, Zaffryar-Eilot S, Holzer A, Ogg S, Thai D, Neufeld G, Van Vlasselaer P, Smith V (2010) Allosteric inhibition of lysyl oxidase-like-2 impedes the development of a pathologic

microenvironment. Nat Med 16(9):1009–1017. https://doi.org/10.1038/nm.2208

67. Loomba R, Seguritan V, Li W, Long T, Klitgord N, Bhatt A, Dulai PS, Caussy C, Bettencourt R, Highlander SK, Jones MB, Sirlin CB, Schnabl B, Brinkac L, Schork N, Chen CH, Brenner DA, Biggs W, Yooseph S, Venter JC, Nelson KE (1062e) Gut microbiome-based metagenomic signature for non-invasive detection of advanced fibrosis in human nonalcoholic fatty liver disease. Cell Metab 25(5):1054–1062e1055. https://doi.org/10.1016/j.cmet.2017.04.001
68. Ikenaga N, Peng ZW, Vaid KA, Liu SB, Yoshida S, Sverdlov DY, Mikels-Vigdal A, Smith V, Schuppan D, Popov YV (2017) Selective targeting of lysyl oxidase-like 2 (LOXL2) suppresses hepatic fibrosis progression and accelerates its reversal. Gut 66(9):1697–1708. https://doi.org/10.1136/gutjnl-2016-312473
69. Raghu G, Brown KK, Collard HR, Cottin V, Gibson KF, Kaner RJ, Lederer DJ, Martinez FJ, Noble PW, Song JW, Wells AU, Whelan TP, Wuyts W, Moreau E, Patterson SD, Smith V, Bayly S, Chien JW, Gong Q, Zhang JJ, O'Riordan TG (2017) Efficacy of simtuzumab versus placebo in patients with idiopathic pulmonary fibrosis: a randomised, double-blind, controlled, phase 2 trial. Lancet Respir Med 5(1):22–32. https://doi.org/10.1016/S2213-2600(16)30421-0